DIFFUSION IN ALUMINUM ALLOYS

BY

ACTIVATION ANALYSIS

A STUDY OF DIFFUSION
IN ALUMINUM-RICH ALLOYS OF
ALUMINUM, COPPER, AND MANGANESE
BY ACTIVATION ANALYSIS

By

GRENVILLE ROBERT MASON, B.A.Sc.

A Thesis
Submitted to the Faculty of Graduate Studies
in Partial Fulfilment of the Requirements
for the Degree
Master of Engineering

McMaster University
September 1959

MASTER OF ENGINEERING(1959)   MCMASTER UNIVERSITY
(Metallurgy)   Hamilton Ontario

TITLE: A Study of Diffusion in Aluminum-rich Alloys of Aluminum, Copper, and Manganese by Activation Analysis

AUTHOR: Grenville Robert Mason, B.A.Sc. (University of British Columbia)

SUPERVISOR: Professor J.S. Kirkaldy

NUMBER OF PAGES: x, 57

SCOPE AND CONTENTS:

In this thesis, the theory is developed for the determination of concentration-dependent diffusion coefficients from experimental data for multi-component systems, and a study is made of the applicability of neutron activation analysis to samples from diffusion couples. Diffusion coefficients have been determined for copper and manganese in a matrix of aluminum by diffusing semi-infinite couples of alloys near the single-phase region at the aluminum rich corner of the ternary diagram for this system. The couples were sectioned on a lathe after the diffusion anneal and samples were analysed by neutron activation and subsequent measurement of the induced gamma radiation.

PREFACE

This work was undertaken to determine the effect of manganese on the rate of diffusion of copper in aluminum in anticipation of possible effects on the precipitation rate of $CuAl_2$ in Al-Cu-Mn alloys. Toward this end,

(a) the theory has been developed for the analysis of concentration-dependent diffusion in multi-component systems,

(b) a method is given for designing experiments to determine the diffusion coefficients for a given system most efficiently,

(c) the method of composition analysis by neutron activation and subsequent measurement of gamma radiation is outlined, its scope and limitations given, and

(d) six different couples of alloys in the Al-Cu-Mn system were diffused, analysed by neutron activation analysis, and the diffusion coefficients calculated.

Activation analysis was used for composition determination for two reasons: first, the samples obtainable from a diffusion couple are small (of the order of ten milligrams); second, the method of activation analysis is relatively new and it was thought desireable to explore the scope and precision of this method. The use of activation analysis seemed particularly appropriate at McMaster University, where Canada's first university experimental reactor has been built. Actually, the main irradiations for this work were made at Brookhaven National Laboratories in Upton N.Y., U.S.A. since the McMaster reactor was not yet fully operational.

ACKNOWLEDGEMENTS

The author is indebted to Dr. J.S. Kirkaldy for suggesting the problem and for his advice and encouragement during the course of this work. Thanks are due to Mr. W.J. Slater for many helpful conversations and for his cooperation in the use of the equipment, and to Dr. W.H. Fleming for providing some preliminary irradiations in the McMaster reactor. Acknowledgement is also made of financial assistance through Annual Grant A697 to Dr. Kirkaldy from the National Research Council of Canada.

TABLE OF CONTENTS

Page

Introduction 1

Diffusion Analysis 4

  Relationships between ternary diffusion coefficients for different reference frames 8

  Representation of concentration-dependent diffusion coefficients 10

  Aids for the construction of ternary diffusion diagrams 10

  Determination of concentration-dependent diffusion coefficients from experimental penetration curves 11

  A special solution for constant coefficients in a ternary system 18

Activation Analysis 20

  Activity as a result of irradiation 21

  Gamma-ray detection 24

  Gamma-ray spectrometer 26

  Counting castle and storage container 28

  Copper and manganese activity 29

Experimental Procedure and Results 33

  Preparation of samples for irradiation 35

  Measurement of activity in samples 37

  Results of activity measurements 41

  Discussion 46

Conclusions 50
Appendix A 51
References 56

LIST OF ILLUSTRATIONS AND DIAGRAMS

After Page:

1. Typical penetration curve for concentration-dependent diffusion in a binary system 6

2. A representation of concentration-dependent diffusion coefficients for a ternary system 10

3. Information from a binary couple 10

4. Information from the requirement that:
$D^{m}_{ik} = 0$ at $C_i = 0$ 10

5. Possible experimental conditions for semi-infinite diffusion couples 14

6. Relationships between C_i and C_k for diffused ternary couples having the initial conditions shown in figure 5 14

7. Quantities to be evaluated for the determination of the four concentration-dependent diffusion coefficients for a ternary system 15

8. Quantities to be evaluated for the determination of the two concentration-dependent diffusion coefficients obtainable when $dC/d\lambda = 0$ at finite λ 15

9. Theoretical over-all photopeak counting efficiency $(g \cdot p)$, as a function of distance, for point sources on the centerline of a 25 millimeter NaI(Tl) crystal 25

10. Spectrum of energies dissipated in a scintillation crystal for mono-energetic gamma radiation 25

11. Actual shape of spectrum produced by a gamma-ray spectrometer 25

12. Gamma-ray spectrometer 26

13. Flow diagram showing the connections between the units of the gamma-ray spectrometer 26

14. Relative counting rates from a given source placed on different shelf positions in the counting castle 29

15. Counting castle 29

16. Storage container 29

17. Spectrum of copper-64 29

18. Spectrum of manganese-56 29

19. 500°C isotherm for the Al-rich corner of the Al-Cu-Mn system 33

20. Binary diagram for aluminum-copper 33

21. Binary diagram for aluminum-manganese 33

22. Extrapolated 556.5°C isotherm for the Al-rich corner of the Al-Cu-Mn system 33

23. Clamp for diffusion couples 34

24. Forced-convection tempering oven used for diffusion anneals 34

25. Diffusion couple temperature 34

26. Silica capsules, irradiation spacer, and sample assemblies 36

27. Spacing of capsules in irradiation container 36

28. Background in samples at the 0.51 Mev copper photopeak 42

29. Background in samples at the 1.8 Mev manganese photopeak 42

30. Copper penetration in the couples 45

31. Effect of manganese gradient on copper diffusion 45

32. Manganese penetration in the couples 45

INTRODUCTION

A diffusion coefficient is a measure of the rate at which one substance moves through another. One of the simpler and more conventional techniques for determining diffusion coefficients in metals is to bring two pieces of metal into intimate contact, to heat the "couple" to a high temperature in order to get a detectable penetration of one metal into the other in a reasonable length of time, to take samples at various distances along the couple and to analyse the composition of these samples. From an analysis of the variation of composition in the two sides of the couple diffusion coefficients can be calculated.

In this paper the theory is developed for the determination of concentration-dependent multi-component diffusion coefficients from experimental measurements, and the applicability of the method of activation analysis to the measurement of diffusion in metal systems is studied. In addition, diffusion coefficients are determined for the diffusion of copper and manganese in aluminum.

The theory developed for the determination of concentration-dependent multi-component diffusion coefficients is an extension of the work initiated by Onsager[1] and developed for metal systems by Darken[2] and Kirkaldy[3-7] and is a generalization of the method of Boltzmann[8] and Matano[9] for binary systems. Except for a special type of diffusion couple it is shown that, in general, more than one diffusion couple must be annealed and analysed before any values can be calculated for the concentration-dependent coefficients; in fact, the maximum number of values that can be obtained for a particular diffusion coefficient of a ternary system equals $(K-1)! + K$, $(K > 1)$, where K is the number of different diffusion couples annealed and analysed.

While the method used in the experiments reported here for diffusing and sectioning the couples was more conventional, the method of composition analysis by neutron activation and subsequent measurement of the induced gamma radiation was comparatively new. The advantage of activation analysis lies in the fact that only very small samples, of the order of ten milligrams, are required with neutron fluxes available (about 10^{13} neutrons/cm^2/sec) in present day reactors to get an accuracy of about one percent. A disadvantage is that not all elements, or combinations of elements can be conveniently analysed by this method.

The accuracy obtainable by activation analysis is better than most analytical methods for samples of the size available in diffusion work. However, analyses using an electron probe micro-analyser[10] are reported to provide about the same degree of accuracy and may prove to be far more convenient for analyses of diffusion couples, when these become more universally available.

The method of activation analysis is particularly well suited for use at McMaster University, where Canada's first university-owned reactor is situated. Unfortunately the reactor was not yet fully operational at the time this work was done so that use had to be made of another reactor. The irradiation facilities of the Brookhaven National Laboratories were found to be most convenient because the neutron flux was suitable and because samples could be transported from this reactor to the McMaster campus with the least delay (usually about twelve hours).

DIFFUSION ANALYSIS

Fick's first "law" of diffusion[11] is the basis for the phenomenological theory of diffusion; for uni-directional dissusion, this law is simply

(1) $$J = -D \frac{\partial C}{\partial x}$$

where J is the diffusion current in concentration units per unit area per unit time

D is the diffusion coefficient in units of area per unit time

C is the concentration

and x is distance

Fick's second law of diffusion is derived from the first by consideration of the rate of accumulation of diffusing substance in a given volume. The second law, for uni-directional diffusion, is

(2) $$\frac{\partial C}{\partial t} = \frac{\partial}{\partial x}\left(D \frac{\partial C}{\partial x}\right)$$

or, for constant D,

(3) $$\frac{\partial C}{\partial t} = D \frac{\partial^2 C}{\partial x^2}$$

For a semi-infinite diffusion couple, the boundary conditions are

$$(4)\quad \begin{cases} C = C^{\circ} & \text{for} \quad 0 < x < \infty,\ t = 0;\ x = \infty,\ \text{all } t \\ C = C' & \text{for} \quad -\infty < x < 0,\ t = 0;\ x = -\infty,\ \text{all } t \end{cases}$$

and the corresponding solution to equation (3) is[12]

$$(5)\quad C = C^{\circ} + \frac{(C' - C^{\circ})}{2}\left(1 - \operatorname{erf}\frac{x}{2\sqrt{Dt}}\right)$$

where $\operatorname{erf}\frac{x}{2\sqrt{Dt}} = \frac{2}{\sqrt{\pi}}\int_{0}^{\frac{x}{2\sqrt{Dt}}} e^{-\xi^{2}}\, d\xi$

Values for the error function (erf) can be obtained from <u>the Handbook of Chemistry and Physics</u>.[13]

In general, however, the diffusion coefficient, D, is not a constant and must be considered as a function of concentration. In this case, the solution to equation (2), for boundary conditions (4), is[8]

$$(6)\quad C = C^{\circ} + (C' - C^{\circ})\,\frac{\displaystyle\int_{\lambda}^{\infty}\frac{d\lambda'}{D(\lambda')}\, e^{-\int_{0}^{\lambda'}\frac{\lambda''\,d\lambda''}{2D(\lambda'')}}}{\displaystyle\int_{-\infty}^{\infty}\frac{d\lambda'}{D(\lambda')}\, e^{-\int_{0}^{\lambda'}\frac{\lambda''\,d\lambda''}{2D(\lambda'')}}}\,, \quad \lambda = \frac{x}{\sqrt{t}}$$

While an assumed-constant diffusion coefficient, D, is determined simply by finding the value of D which will make solution (5) best fit the experimental results, the Boltzmann-Matano analysis must be used when D is a function of concentration. Here, the relation

$$(7) \qquad D = \frac{-\frac{1}{2}\int_{C^0}^{C} \lambda \, dC}{dC/d\lambda}$$

is used in evaluating D from a diffusion penetration curve such as that shown in figure 1. It is to be noted that the Matano interface, the origin for the distance axis as shown, must be so chosen that the two shaded areas are equal. Whenever a component on one side of a couple diffuses faster than that on the other, and the diffusion is not interstitial, then the original interface will move relative to the ends of the couple. The Matano interface will correspond to the original position of the interface. The movement of the original interface, or weld, is known in metal diffusion as the "Kirkendall effect"[14].

While the above analyses may be adequate for binary diffusion, complications arise in multi-component diffusion due to the presence of other constituents and due to concentration gradients of other constituents. To allow for these complications Onsager[1] suggested the extension of equation (1),

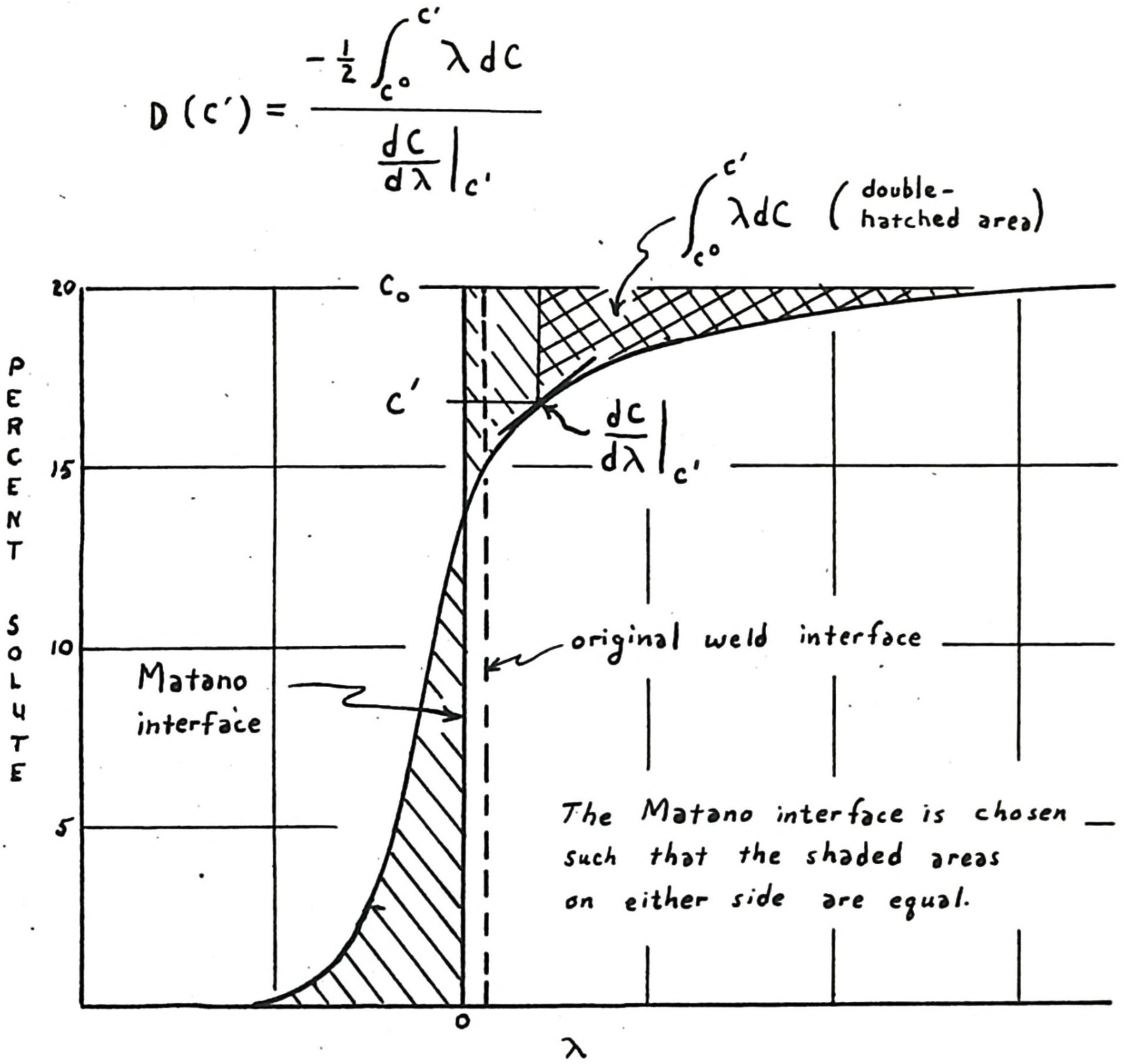

<u>Figure 1</u> Typical Penetration Curve for Concentration-dependent Diffusion in a Binary System

(8) $$J_i = -\sum_k D'_{ik} \frac{\partial C_k}{\partial x} \qquad (i = 1, 2, \cdots n)$$

A number of authors have considered the application of this extension to metal systems, notably Darken[2] and Kirkaldy[3-7].

In substitutional alloys, volume changes of mixing and conservation of lattice sites can usually be assumed. Thus, the diffusion currents, when referred to a stationary lattice outside the diffusion zone, are linearly related by the equation:

(9) $$\sum_{i=1}^{n} J_i = 0$$

If, in addition, the concentrations are in such units that

(10) $$\sum_{i=1}^{n} C_i = \text{constant}$$

then the system of equations given by (8) can be reduced to (n-1) equations each involving only (n-1) coefficients:

(11) $$J_i = -\sum_{k=1}^{n-1} D_{ik} \frac{\partial C_k}{\partial x} \qquad (i = 1, 2, \cdots n-1)$$

where $D_{ik} = D'_{ik} - D'_{in}$

For a three-component system, then,

$$(11a)\quad \begin{cases} J_1 = -D_{11}\dfrac{\partial c_1}{\partial x} - D_{12}\dfrac{\partial c_2}{\partial x} \\ J_2 = -D_{21}\dfrac{\partial c_1}{\partial x} - D_{22}\dfrac{\partial c_2}{\partial x} \end{cases}$$

Here, there are only four independent coefficients, D_{11}, D_{12}, D_{21}, and D_{22} which have been obtained from an initial total of nine for a three-component system by the use of equations (9) and (10).

An exact solution of the equations for free diffusion in three-component systems with interacting flows has been found by Fujita and Gosting[15] for constant diffusion coefficients; and a general theorem for construction of multi-component solutions from solutions of the binary diffusion equation has been given by Kirkaldy[7], again for constant diffusion coefficients. In a later section a method is given for evaluating from experimental data concentration-dependent diffusion coefficients for multi-component systems.

Relationships between ternary diffusion coefficients for different reference frames

In the foregoing, no restriction has been placed upon the diffusion coefficients; in general, they are not constant and can be considered to be dependent upon the concentrations of (n-1) constituents.

Concentration-dependent diffusion coefficients can theoretically be determined for the whole range of compositions of an alloy system. Since the component which is present in the greatest amount is usually considered as the matrix, or nth component, then data for the same alloy system may be compiled using different sets of diffusion coefficients, as required for equation (11). It would be desireable to have a knowledge of the variation of a particular set of diffusion coefficients over the complete range of compositions of a system. For this reason, it would probably be necessary to transfer data from experiments in which one component was considered as the matrix element to a diagram or set of data for which a different component was considered as the matrix element. The equations required for such a transfer of data can be obtained by simple, even if perhaps lengthy, algebra from equations (8), (9), (10), and (11), as shown for a ternary system in Appendix A. For a ternary system, writing a super-postscript with the diffusion coefficients to denote the solvent component, the diffusion coefficients for different choices of solvent are related as follows:

$$(12) \qquad D^{m}_{ik} = D^{k}_{mm} - D^{m}_{kk} = D^{m}_{ii} - D^{k}_{ii} = -D^{k}_{im}\,,$$

$$i,\ k,\ m \quad \text{all different}$$

The set of equations (12) is sufficient for the transfer of data in which k is taken as the solvent component to data in which m is the solvent component. (It is useful to remember that D_{ik}^{m} refers to the diffusion of component i down the gradient of component k, when the solvent component is m.)

Representation of concentration-dependent diffusion coefficients

For a ternary system it would be convenient to represent the values for any particular diffusion coefficient on an isothermal ternary diagram of the type normally used to show the different phases for a ternary system. Four such diagrams are needed, one for each of four coefficients, to completely describe diffusion in a ternary system. A hypothetical diagram is shown as figure 2. Discontinuities in the diffusion coefficients are to be expected at phase changes, although none have been indicated in figure 2.

Aids for the construction of ternary diffusion diagrams

The binary diffusion coefficient gives the value for the ternary diffusion coefficient along an edge of a ternary diagram for an on-diagonal diffusion coefficient. This conclusion should be self-evident from figure 3.

It should also be evident that when the concentration of a component goes to zero its current also vanishes so that its off-diagonal coefficient must go to zero.

Figure 2 A Representation of Concentration-dependent Diffusion Coefficients for a Ternary System

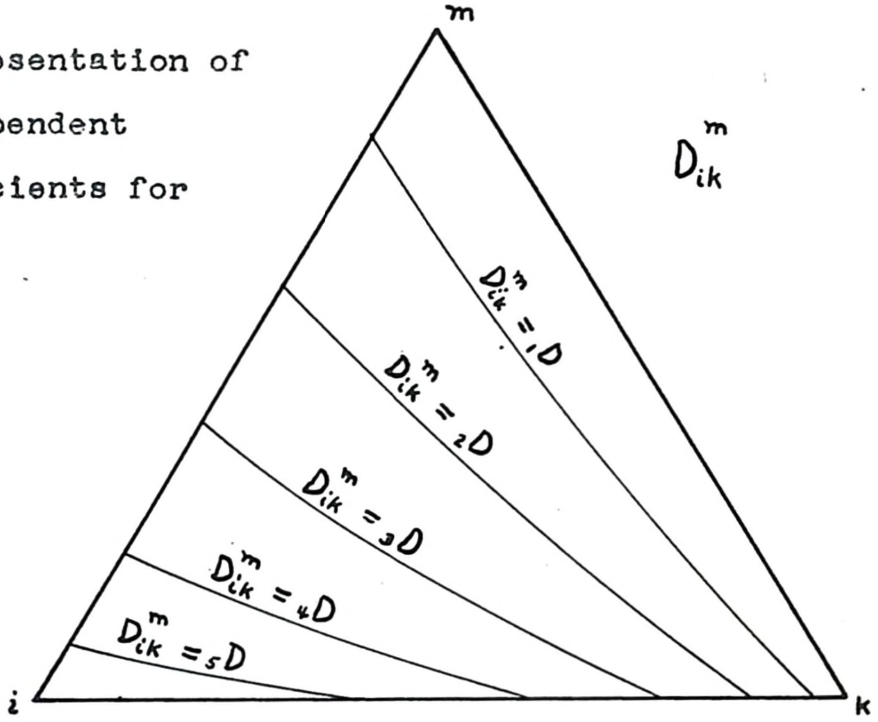

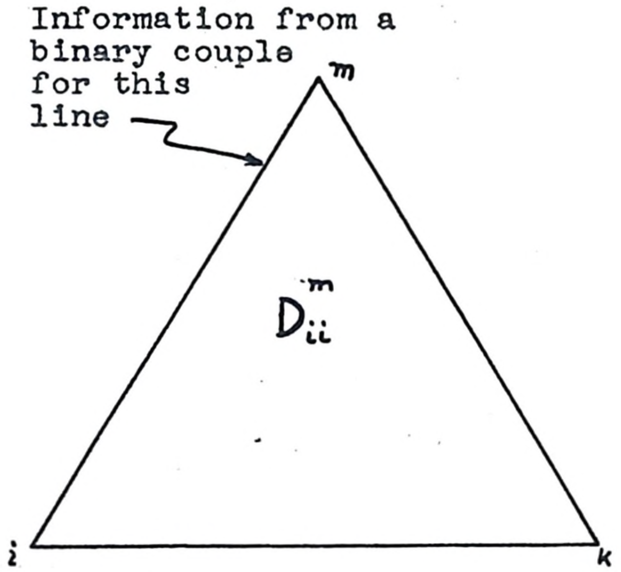

Figure 3 Information from a Binary Couple

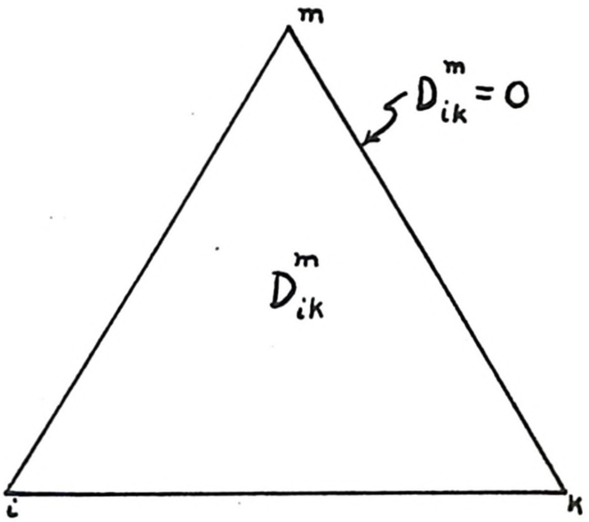

Figure 4 Information from the Requirement that $D_{ik}^m = 0$ at $C_i = 0$

For example, referring to equation (11a), whenever C_1 is zero, J_1 must also be zero; the first term on the left side of equation (11a) is zero if C_1 is zero but the second term is always zero only if D_{12} is zero. This is shown in figure 4.

Determination of concentration-dependent diffusion coefficients from experimental penetration curves

For each component of a multi-component system the continuity equation is valid:

$$\frac{\partial J_i}{\partial x} + \frac{\partial C_i}{\partial t} = 0 \tag{13}$$

On substituting equations (11) into equations (13) one obtains (n-1) simultaneous diffusion equations of the form

$$\frac{\partial C_i}{\partial t} = \sum_{k=1}^{n-1} \frac{\partial}{\partial x} \left[D_{ik} \frac{\partial C_k}{\partial x} \right] \tag{14}$$

By analogy with the Boltzmann-Matano analysis for binary diffusion with concentration dependent coefficients, parametric solutions are sought having the form

$$C_i = C_i(\lambda) , \quad \lambda = x/\sqrt{t} \tag{15}$$

By combining (15) with (14) the set of non-linear ordinary differential equations

$$(16)\qquad -\frac{\lambda}{2}\frac{dC_i}{d\lambda} = \sum_{k=1}^{n-1}\frac{d}{d\lambda}\left[D_{ik}\frac{dC_k}{d\lambda}\right]$$

is obtained.

Equations (16) can be applied to a semi-infinite diffusion couple for which the initial conditions are

$$(17)\qquad \begin{cases} C_i = C_i^0 & \text{for } x>0 \text{ and } t=0 \quad (i.e.,\ \lambda=\infty) \\ C_i = C_i' & \text{for } x<0 \text{ and } t=0 \quad (i.e.,\ \lambda=-\infty) \end{cases}$$

From a first integration of equation (16), then,

$$(18)\qquad \int_{C_i^0}^{C_i}\lambda\, dC_i = -2\sum_{k=1}^{n-1} D_{ik}\frac{dC_k}{d\lambda}$$

Since one can determine the value of the integral and of the slopes $dC_k/d\lambda$ from measured experimental curves, then equations (18) together with experimental data can be used for the determination of the concentration-dependent diffusion coefficients. In binary alloys the procedure is the standard Boltzmann-Matano analysis and is relatively easy to carry out since there is only one coefficient to be determined from one penetration curve. For diffusion in higher-order alloys the mathematical analysis is much more complicated and the amount of experimental data required is much greater. The procedure to be followed in order to determine concentration-dependent diffusion coefficients for a three-component system is outlined below; for higher order systems the procedure would be similar but more complicated.

For $n=3$ equation (18) may be written

$$(18a) \quad \int_{C_1^0}^{C_1} \lambda \, dC_1 = -2 D_{11} \frac{dC_1}{d\lambda}\bigg|_{C_1} - 2 D_{12} \frac{dC_2}{d\lambda}\bigg|_{C_1}$$

and

$$(18b) \quad \int_{C_2^0}^{C_2} \lambda \, dC_2 = -2 D_{21} \frac{dC_1}{d\lambda}\bigg|_{C_2} - 2 D_{22} \frac{dC_2}{d\lambda}\bigg|_{C_2}$$

where the coefficients all have the form $D = D(C_1, C_2)$. In general, the two penetration curves obtained from a single diffusion couple are not sufficient to determine even a single value for each of the coefficients since for a given combination of C_1 and C_2 only two equations can be obtained for four unknown quantities. It is necessary therefore to have measured penetration curves for more than one couple and each couple must have different initial conditions if values for the concentration-dependent diffusion coefficients are to be determined. Provided the initial conditions have been properly chosen for two couples (some overlap in the ranges of concentrations) identical sets of concentrations will be found in each of the two couples, at different values of λ . By evaluating $\int_{C_1^0}^{C_1} \lambda \, dC_1$ up to this value of λ , and $\frac{dC_1}{d\lambda}$ and $dC_2/d\lambda$ at this value of λ , then an equation containing $D_{11}(C_1, C_2)$ and $D_{12}(C_1, C_2)$ can be obtained for each couple; hence

$D_{11}(c_1, c_2)$ and $D_{12}(c_1, c_2)$ can be determined. $D_{21}(c_1, c_2)$ and $D_{22}(c_1, c_2)$ can be evaluated in the same way.

Figure 5 shows five different possible experimental combinations for semi-infinite diffusion couples, with both the initial conditions and the conditions after some time, t, illustrated. In order to determine the sets of concentrations for which concentration and dependent diffusion coefficients can be calculated, it is necessary to plot the concentration of one component as a function of the concentration of a second for the length of a couple. For example, the conditions after some time, t, shown in figure 5, are plotted in figure 6. It is noted that curves 2 and 3 intersect at the point (C_i', C_k'). This set of concentrations is that for which all four diffusion coefficients can be calculated by the method described in the previous paragraph. The quantities which must be evaluated for the determination of the four diffusion coefficients are illustrated in figure 7.

Each succeeding couple which is diffused with different initial conditions can give another set of values for the coefficients for each couple that has already been diffused, provided the initial conditions are suitable. Thus, the number of values which can normally be obtained for each of the diffusion coefficients of a ternary system equals $(K-1)!$, $(K > 1)$, where K is the number of couples which have been diffusion-annealed,

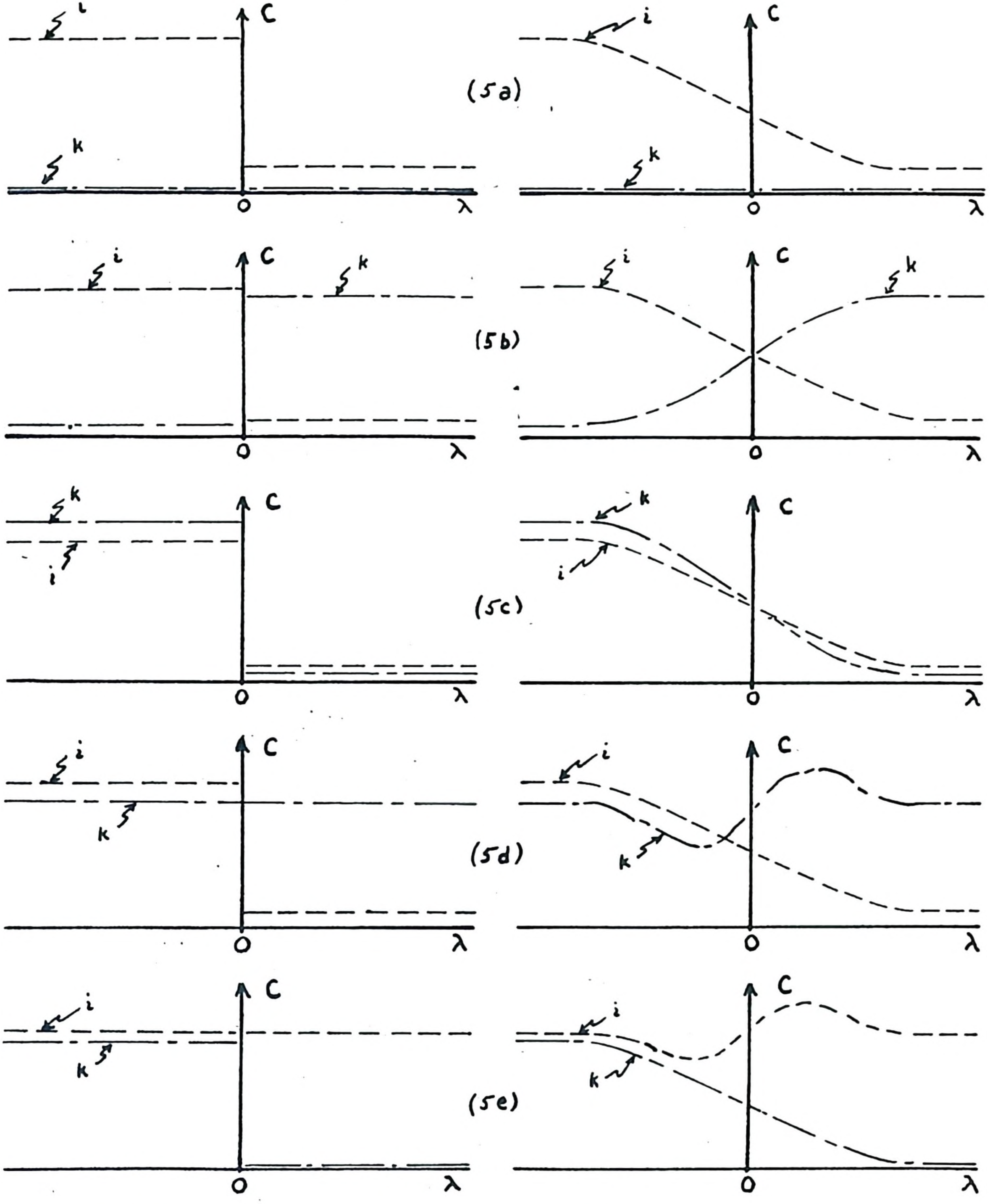

Initial Conditions   Conditions after some time t

Figure 5 Possible Experimental Conditions for Semi-infinite Diffusion Couples

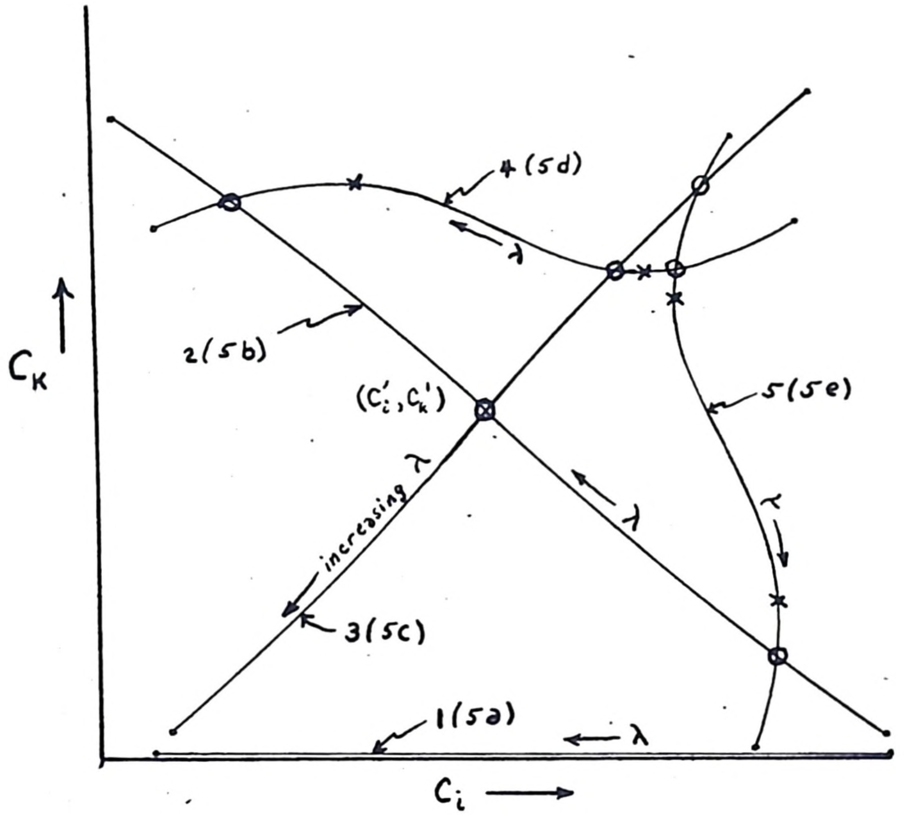

Where curves cross, or when $dC_i/dC_K = 0$ (or ∞), then concentration-dependent diffusion coefficients can be determined.

o indicates a set of concentrations for which all four diffusion coefficients can be determined.

x indicates a set of concentrations for which two diffusion coefficients can be determined. (If $dC_K/dC_i = 0$ then D_{ii} and D_{ki} can be calculated; if $dC_i/dC_k = 0$ then D_{ik} and D_{kk} can be calculated.

Figure 6 Relationships between C_i and C_K for diffused ternary couples having the initial conditions shown in figure 5.

and which had appropriate, different initial conditions.

Information in addition to that outlined above can be obtained from a special type of diffusion couple in which the initial concentration of one non-matrix component is the same on both sides of a couple while the initial concentration of the other non-matrix component changes suddenly at the interface (see curves 5d and 5e of figure 5). Provided there is a measurable cross-effect, the steep gradient of the one component will force the other component across the interface and the initially-constant distribution will assume an S-shape. By choosing the upper limit of integration in equations (18a) and (18b) so that it corresponds to one of the finite values of λ where the concentration gradient of the one component is zero, then one diffusion coefficient can be evaluated from each equation for each of the two points where the gradient is zero at finite λ.

For example, an enlarged diagram of curve 5d of figure 5, showing the quantities to be evaluated for this special case, is shown as figure 8. At (c_1', c_2'), where $dc_2/d\lambda$ is zero for a finite value of λ, then from equations (18a) and (18b):

$$(19a) \qquad \int_{c_1^0}^{c_1'} \lambda \, dc_1 = -2D_{11} \left. \frac{dc_1}{d\lambda} \right|_{c_1'}$$

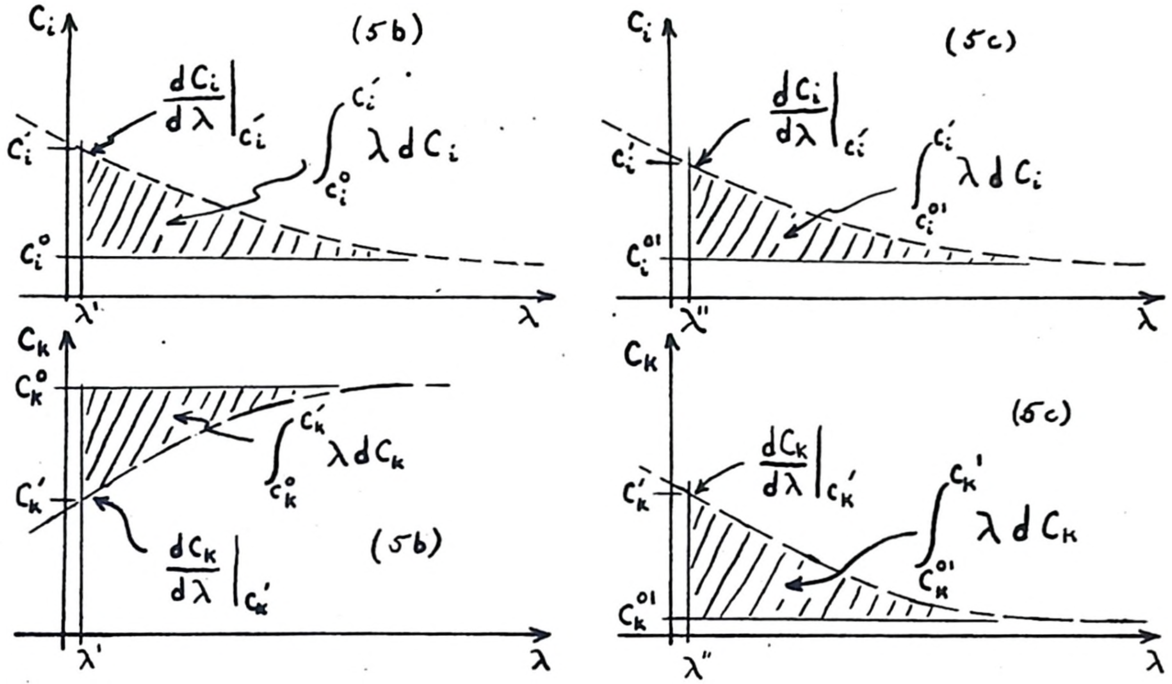

Figure 7 Quantities to be evaluated for the determination of the four concentration-dependent diffusion coefficients for a ternary system (see equation 18 and figure 5)

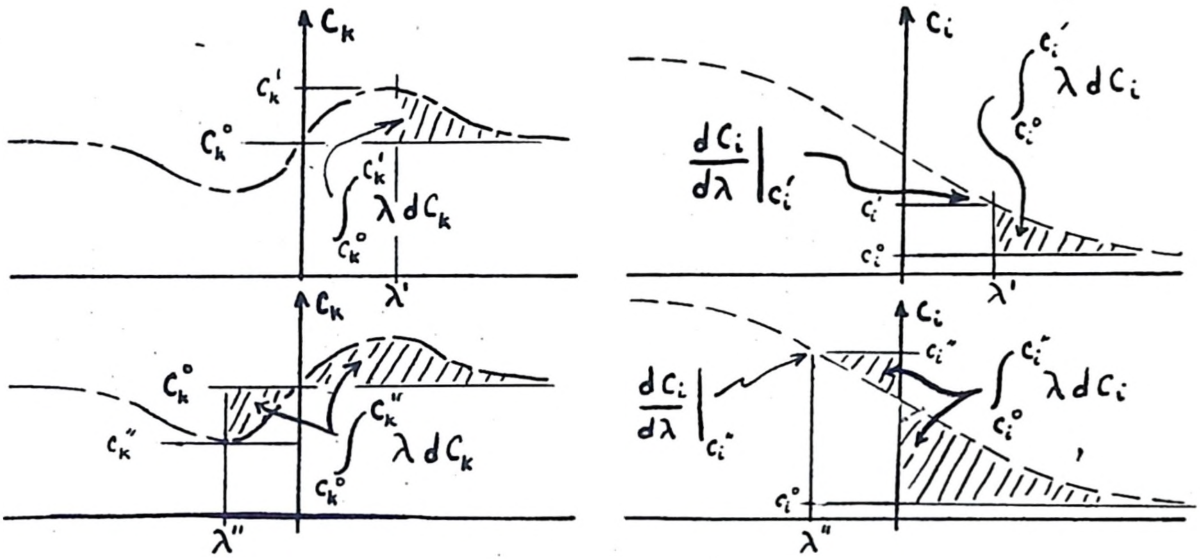

Figure 8 Quantities to be evaluated for the determination of the two concentration-dependent diffusion coefficients obtainable when $dc/d\lambda = 0$ at finite λ.(see equation 19 and figure 5d)

and

$$(19b) \qquad \int_{C_2^{\circ}}^{C_2'} \lambda \, dC_2 = -2 D_{21} \left.\frac{dC_1}{d\lambda}\right|_{C_2'}$$

These equations can also be evaluated for (C_1'', C_2'') so that two values for each of two coefficients can be evaluated in this special case. Thus, in addition to the (K-1)! values, (K > 1), that can normally be obtained for each diffusion coefficient from K couples, a maximum of K more values for each coefficient, on the average, can be had from these special couples.

It will not be known initially for what combinations of concentrations the diffusion coefficients will be determined. However, an approximate idea can be obtained by plotting on a rectangular plot the initial concentrations of one component against the other. A straight line drawn between the points representing the initial concentrations on either side of the couple will show the approximate trend in the concentrations at some later time. The intersection of such lines will give the approximate concentrations for which the coefficients can be calculated.

An exact analysis for concentration-dependent coefficients is possible only for individual sets of concentrations. Therefore, to describe variations in the diffusion coefficient over a whole range of concentrations it would be necessary to fit analytical expressions to the experimental data. One such analytical expression, however, could almost be assumed because of the physical necessity that D_{ik} go to zero as C_i goes to zero; this expression would be

$$D_{ik} = d_{ik} C_i \,, \qquad d_{ik} \text{ constant} \tag{20}$$

Under this assumption equations (18a) and (18b) become

$$\int_{C_1^0}^{C_1} \lambda \, dC_1 = -2 D_{11} \left.\frac{dC_1}{d\lambda}\right|_{C_1} - 2 d_{12} C_1 \left.\frac{dC_2}{d\lambda}\right|_{C_1} \tag{21a}$$

and

$$\int_{C_2^0}^{C_2} \lambda \, dC_2 = -2 d_{21} C_2 \left.\frac{dC_1}{d\lambda}\right|_{C_2} - 2 D_{22} \left.\frac{dC_2}{d\lambda}\right|_{C_2} \tag{21b}$$

Two couples with appropriate initial conditions are all that are necessary for the determination of the four unknown quantities in equations (14a) and (14b). Then, once d_{12} and d_{21} have been found, a line of values for each of D_{11} and D_{22} can be determined from each couple. Either d_{12} or d_{21} could be found from just one single-step couple; and, in fact, two values can be found for one of these from just one couple so that the assumption $D_{ik} = d_{ik} C_i$ could be verified or disproved. However, if the assumption $D_{ik} = d_{ik} C_i$ must be rejected then it would be possible to fit D_{ik} to a parabolic function of C_i using the two points determined for D_{ik} and the requirement that $D_{ik} = 0$

when $C_i = 0$. D_{kk} could now be determined under this assumption.

A special solution for constant coefficients in a ternary system

For couples of the type shown in figure 5 (curves d and e) a special solution has been given by Kirkaldy[3] for the assumptions

(a) constant coefficients

(b) $D_{21} \frac{d^2C_1}{d\lambda^2} \ll D_{22} \frac{d^2C_2}{d\lambda^2}$

Applying these assumptions, equations (16) become

$$-\frac{\lambda}{2}\frac{dC_1}{d\lambda} = D_{11}\frac{d^2C_1}{d\lambda^2} + D_{12}\frac{d^2C_2}{d\lambda^2} \tag{22}$$

and

$$-\frac{\lambda}{2}\frac{dC_2}{d\lambda} = D_{22}\frac{d^2C_2}{d\lambda^2} \tag{23}$$

For initial conditions given by (17), equation (23) has the independent solution

$$C_2 = C_2^0 + \frac{C_2' - C_2^0}{2}\left[1 - \mathrm{erf}\frac{\lambda}{2\sqrt{D_{22}}}\right] \tag{24}$$

The substitution of this result into equation (22) yields the solution

(25) $$C_1 = \frac{C_1^0 + C_1^1}{2} + A\left[\operatorname{erf}\frac{\lambda}{2\sqrt{D_{22}}} - \frac{2A - C_1^0 + C_1^1}{2A}\operatorname{erf}\frac{\lambda}{2\sqrt{D_{11}}}\right]$$

where $$A = \frac{D_{12}}{D_{11} - D_{22}} \quad \frac{C_2^1 - C_2^0}{2}$$

ACTIVATION ANALYSIS

Most materials, when placed in a nuclear reactor, become measurably radioactive through the absorption of thermal neutrons. Since the activity of a given sample is proportional to the neutron flux and to the amount of radioactive isotope in the sample it is possible to calculate the amount of isotope which is present in a sample from a measure of its activity. However, because of rather large uncertainties in the neutron flux at a given position of a reactor and in the over-all counting efficiency of a given radiation detector, an accurate calculation is not possible. Consequently, it is necessary to use samples of known composition as standards to determine what amount of activity is to be expected from a given amount of isotope irradiated in a particular position in a reactor and measured for activity under specified conditions. By irradiating samples of unknown composition in positions between those of standard samples the unknown compositions can be determined from a comparison of the activities of the unknown samples with those of the standards. This, then, is the method of activation analysis which is outlined in detail below.

Activity as a result of irradiation

The reaction for the absorption of a thermal neutron by an isotope may be written as

$$(26) \quad {}_{z}I^{P} + {}_{0}n^{1} \longrightarrow {}_{z}I^{P+1} + E$$

where ${}_{z}I^{P}$ represents a particular isotope of an element

Z is the atomic number of the element

P is the number of nucleons in the original isotope nucleus

${}_{0}n^{1}$ represents a neutron

and E is the energy emitted, usually as a "capture" gamma ray, at the time of the reaction.

If the product isotope, I^{P+1}, is radioactive then a measure of this radioactivity is a measure of the amount of the isotope originally present.

The rate at which reaction (26) takes place is proportional to the number of isotope atoms present, N, and to the thermal neutron flux, ϕ, at the position of the isotope atoms in the reactor. The reaction is characterized by a thermal neutron cross section, σ, such that

$$(27) \quad \text{Rate of production of } I^{P+1} = \sigma \phi N$$

If isotope I^{P+1} is radioactive then it will decay at a characteristic rate given by

$$(28) \quad \text{Rate of decay of } I^{P+1} = \lambda N'$$

where N' represents the number of atoms of isotope I^{P+1} present

λ is the disintegration constant for I^{P+1}

Thus, while the element is in the reactor the net increase in the number of atoms of I^{P+1} is

$$\frac{dN'}{dt} = \sigma\phi N - \lambda N' \tag{29}$$

and simply

$$\frac{dN'}{dt} = -\lambda N' \tag{30}$$

when the element is removed.

For a particular position in a reactor, the flux may be assumed constant; σ is constant for a given flux; λ is a characteristic constant; and N is also essentially constant - so that the solutions to equations (29) and (30) are

$$N'(t') = \frac{\sigma\phi N}{\lambda}\left(1 - e^{-\lambda t'}\right) \tag{31}$$

and

$$N'(t) = N'(t_0)\, e^{-\lambda t} \tag{32}$$

where t' is the time as measured from the instant the element is subjected to the neutron flux ϕ

t_0 is the time when the element is removed from the flux

and t is the time as measured from t_0

The activity of an element after removal from a reactor is, then,

$$(33)\quad A = -\frac{dN'}{dt} = \lambda N' = \sigma \phi N (1 - e^{-\lambda t_0}) e^{-\lambda t}$$

It is to be noted that the activity from an irradiated sample is proportional both to the amount of an element present and to the neutron flux. Thus, a measure of activity can be used either to determine neutron flux when it is known how much of an element is present in a sample, or to determine the amount of an element which is present when the flux is known. By using samples of known composition to determine the flux distribution, or, more conveniently, the activity to be expected from a given amount of an isotope, throughout an irradiated assembly then the composition of unknown samples in the assembly can be calculated.

Not all the activity from a sample will be detected however. Only a small fraction, g, of the gamma rays emitted by a sample will even hit the detecting crystal and only a fraction, p, of these will be completely absorbed. A further reduction in the observed counting rate results because gamma radiation of a particular energy is emitted in only a fraction, f, of the disintegrations of an active isotope. If it is assumed that all the gamma rays which are completely absorbed by a crystal are counted then the observed count rate, C will be:

$$C = A f g P \tag{34}$$

Values are given in figure 9 for the product g.p as a function of distance from the detecting crystal for a 25 millimeter sodium iodide crystal, with gamma energy as a parameter. These curves were extrapolated from theoretical data calculated by Miller, Reynold and Snow[16] for larger sized crystals. Although the extrapolation may be inaccurate it is useful nevertheless for estimating the counting rates to be expected from a sample.

Gamma-ray detection

There are several ways in which gamma rays interact with an absorbing material; three of these are important, namely, the photoelectric effect, the Compton effect and pair production. In the photoelectric effect, a gamma ray with energy greater than the binding energy of an orbital electron in an atom interacts with the electron in such a way that the whole of the gamma-ray energy is transferred to the electron. The photoelectric effect thus leads to the complete absorption of the gamma ray. In the Compton process, a gamma ray makes an elastic collision with an outer electron of an atom and gives up a portion of its energy to this electron. Pair production can occur when a gamma ray with energy in excess of 1.02 Mev (million electron volts) passes near a nucleus; it can be annihilated in the strong electrical field of the nucleus with the formation of an electron-positron pair. Pair production usually results in the complete absorption of the gamma ray. At low energies the photoelectric effect is the main absorption process involved; at medium energies the Compton effect is preponderent, while at very high energies, pair production plays the most important role.

When a gamma ray hits a scintillation crystal, whatever energy is absorbed is converted into light impulses. These light impulses can be made to fall upon the cathode of a photomultiplier tube for primary amplification. By applying the output from the photomultiplier tube to a cathode follower, negative voltage pulses will be obtained which are proportional to the amount of gamma ray energy absorbed by the detecting crystal. These negative voltage pulses can then be passed on to a linear amplifier and finally to a pulse height analyser for counting.

If the distribution of energies dissipated in a scintillation crystal is investigated the spectrum obtained for monoenergetic gamma radiation would appear similar to that shown in figure 10. The photoelectric effect, and any combination which results in a total absorption of the energy of the incident photons will give rise to line A, which is known as the photoelectric line. Compton absorption gives rise to a continuous

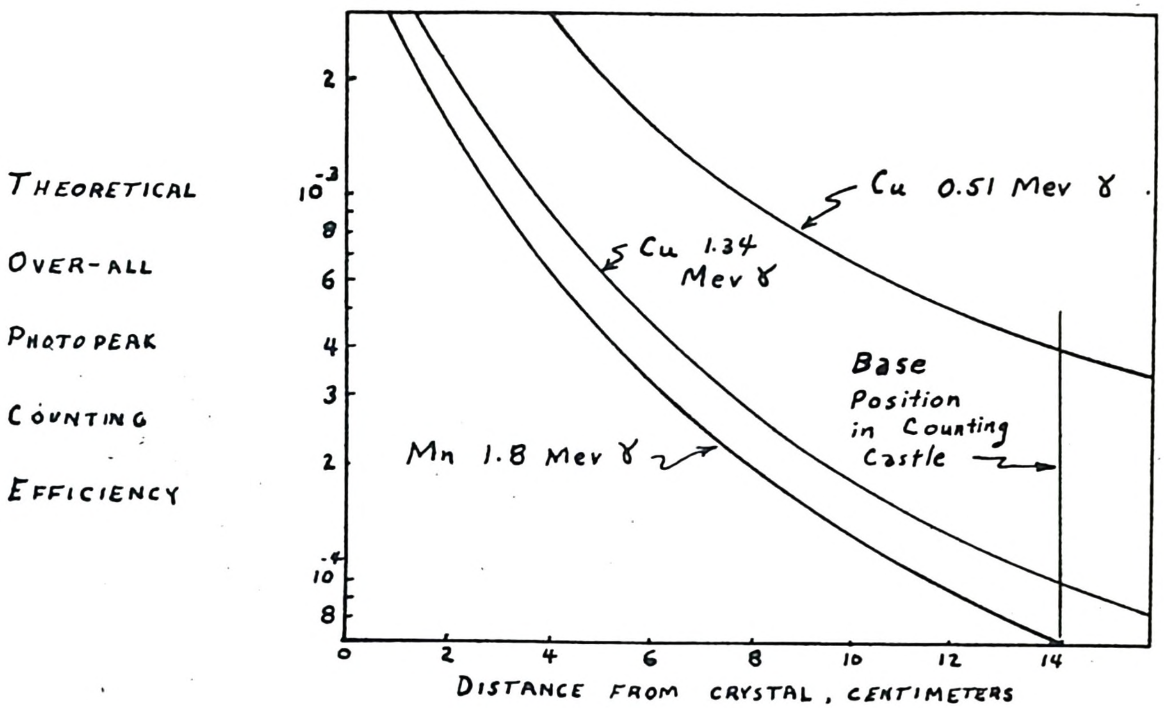

Figure 9 Theoretical over-all photopeak counting efficiency, g.p, as a function of distance, for point sources on the center-line of a 25 millimeter NaI(Th) crystal.

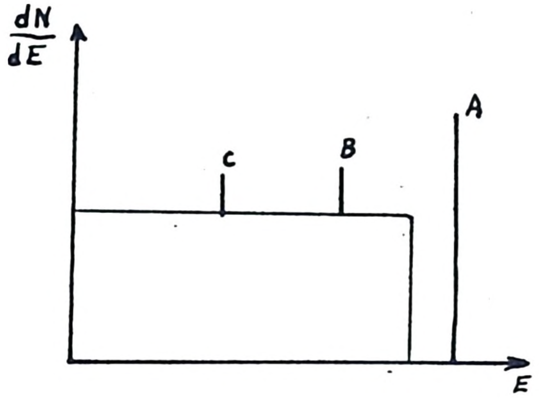

Figure 10 Spectrum of energies dissipated in a scintillation crystal for mono-energetic gamma radiation.

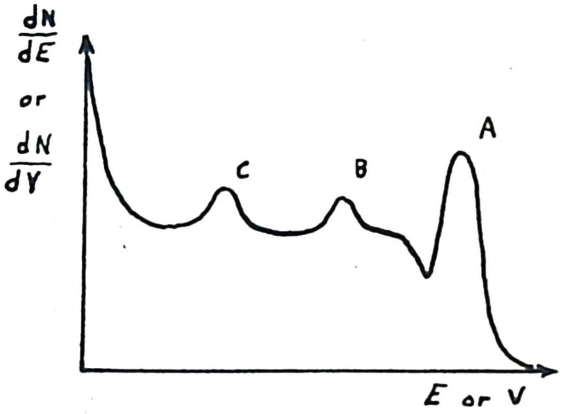

Figure 11 Actual shape of spectrum produced by a gamma ray spectrometer.

spectrum of pulses, indicated by the shaded area of figure 10, whose energies lie between zero and a maximum value which is less than the energy of the initial gamma ray. When the energy of the gamma radiation is at least 1.02 Mev then pair production will occur and two lines, B and C, will arise corresponding to the loss in the crystal of one or both photons produced from annihilation of the positron produced by the pair production.

Since photoelectric emission and secondary emission, the processes which occur in a photomultiplier tube, are statistical phenomena the amplified spectrum corresponding to that shown in figure 10 will be smoothed out. The actual form of the measured spectrum produced by a scintillation counter would look more like figure 11. The broadened peaks corresponding to lines A, B, and C of figure 10 are called photopeaks and the quantity,p, used in equation 34 is the ratio of the number of gamma rays which give rise to a pulse within a photopeak to the total number which interact with the detecting crystal.

Gamma-ray Spectrometer

The apparatus used to measure the gamma activity from samples was a spectrometer purchased from Philips Industries Limited. A picture of the apparatus is shown as figure 12 and a diagram showing the electrical connections is given in figure 13. The components are:

1. PW 4111, a scintillation probe consisting of

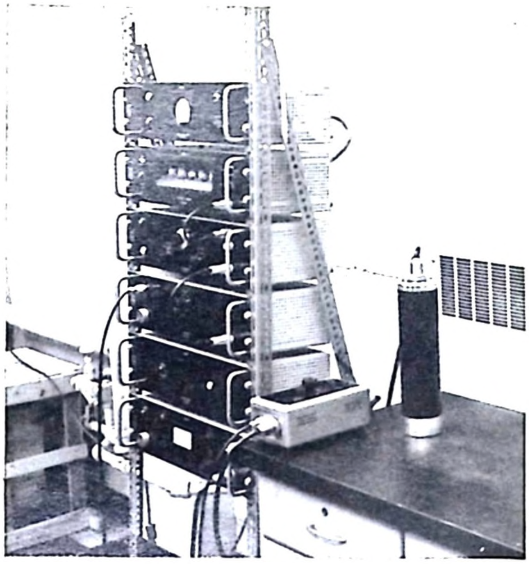

Figure 12 Gamma-ray Spectrometer. The scintillation probe and preamplifier are shown on the table. The mounted units are, from bottom to top: high voltage supply, linear amplifier, pulse height analyser, scaler, and preset-count unit.

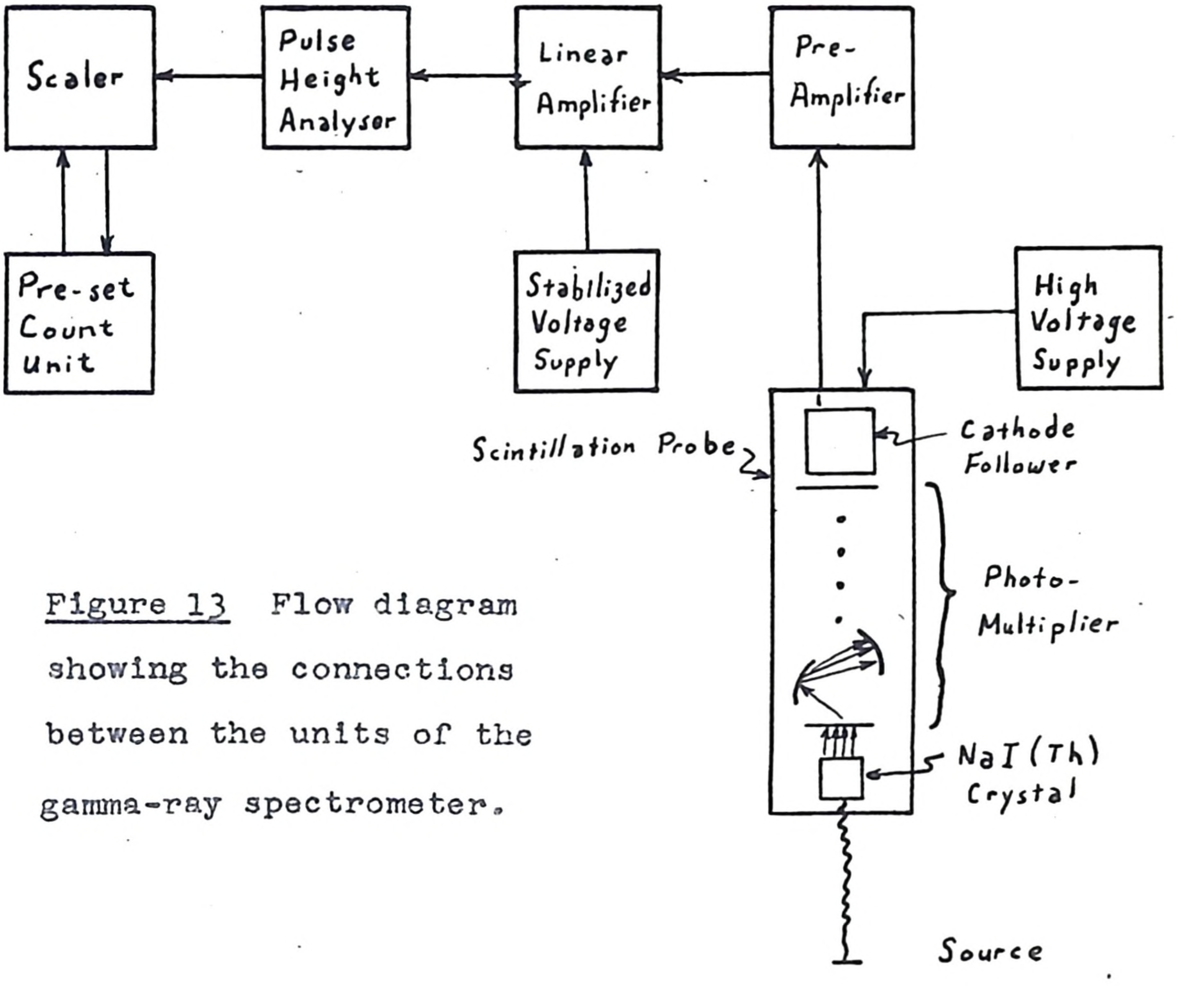

Figure 13 Flow diagram showing the connections between the units of the gamma-ray spectrometer.

a 25 millimeter diameter scintillation crystal (thallium activated sodium iodide) for detecting the radiation, a photomultiplier tube with 11 dynodes, and a cathode follower.

2. PW 4071, a pre-amplifier designed as a link between the radiation detector PW 4111 and the main amplifier PW 4072; it ensures the lowest possible susceptibility to interference of the measuring arrangement.

3. PW 4022, a high-voltage/pre-amplifier unit of which only the high-voltage part was used. The high-voltage section supplies the voltage needed by the radiation detector, PW 4111, up to 2500 volts.

4. PW 4029, a stabilized supply unit designed primarily to supply the power required for the linear amplifier PW 4072. The unit was designed so that it had an output with a variation less than 0.01 per cent of the mains voltage fluctuation.

5. PW 4072, a linear amplifier specially designed for the amplification of pulses with varying amplitude, such as those produced by a scintillation detector. The unit amplifies pulses by the quotient of a constant factor 2400 and of a variable attenuation 1, 2, 4, 8 or 16.

6. PW 4082, a single channel pulse height analyser to separate pulses with different amplitudes

and, thus, to analyse the energy spectrum of radiation. With this instrument, two types of measurement can be made. On threshold discrimination, all pulses are counted which are greater than whatever voltage is set on the instrument. Using channel discrimination all pulses whose size lies within a set range of voltages are recorded. The extent of the range of voltages counted is called the channel width and is adjustable to 1, 2, 4, 8, 12, 16, 20, 24, 28 or 32 volts. The center of the voltage range is called the channel height and is adjustable to any value between 4 and 100 volts.

7. PW 4032, a universal scaler, used for counting pulses up to a maximum count of 400,000. Settings for total counts are 1, 2, or 4 times 10, 100, 1000, 10,000 or 100,000.

8. PW 4072, a preset-count unit, used for measuring the time during which a predetermined number of pulses occur.

Counting Castle and Storage Container

The sample whose activity was to be counted was placed on a shelf inside a lucite box which was in turn fixed inside of a 2-inch-wall lead castle. The scintillation probe projected through a hole in the top of the lead castle and sat on a ridge just above the lucite box. Fourteen shelf positions were available in the lucite box, enabling the sample to be placed at distances of from

0.5 to 14 centimeters from the scintillation crystal. The relative count rates for different shelf positions were determined experimentally and the result is shown as figure 14.

Another 2-inch-wall lead container was made and used for storing samples when their activity was not being measured. Pictures of the counting castle and of the storage container are shown as figures 15 and 16.

Copper and Manganese Activity

Nuclear data for the isotopes of copper and manganese whose activity was measured for the composition analysis is shown in Table 1; and gamma spectra, determined from large samples irradiated in the McMaster reactor at a flux of about 10^9 n/cm^2 - sec are shown in figures 17 and 18 for copper and manganese.

It is noted first that the copper spectrum ends very abruptly above the 1.35 Mev photopeak. By making measurements of the higher energy gamma radiations of the manganese activity then any possible interference from the copper is avoided. Since manganese has a half-life of only 2.58 hours compared with a 12.8 hour half-life for copper, by waiting approximately one day for the manganese activity to decay the copper activity can be measured without appreciable interference. Thus the determination of the amount of copper and manganese in the same alloy can be conveniently made using activation

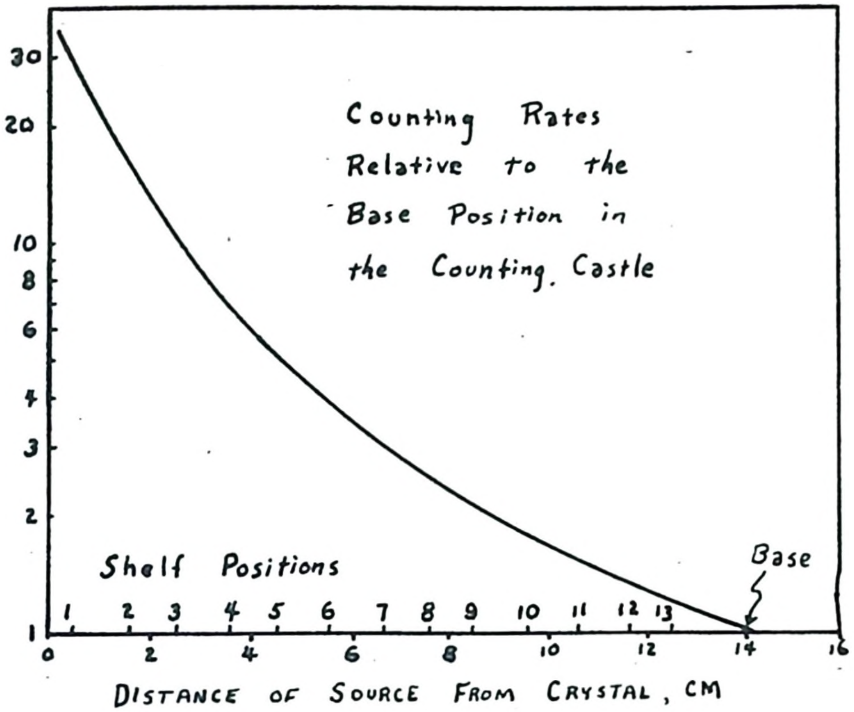

Figure 14 Relative counting rates from a given source placed on different shelf positions in the counting castle.

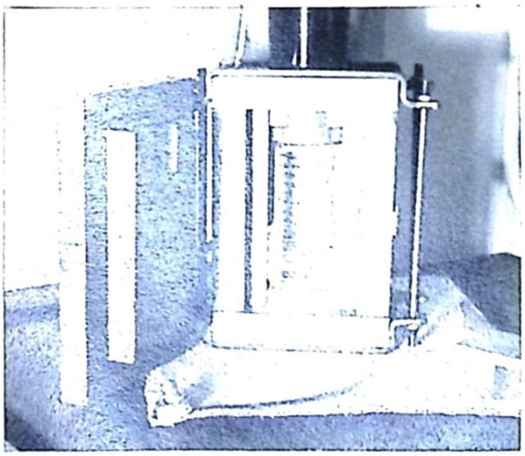

Figure 15 Counting Castle

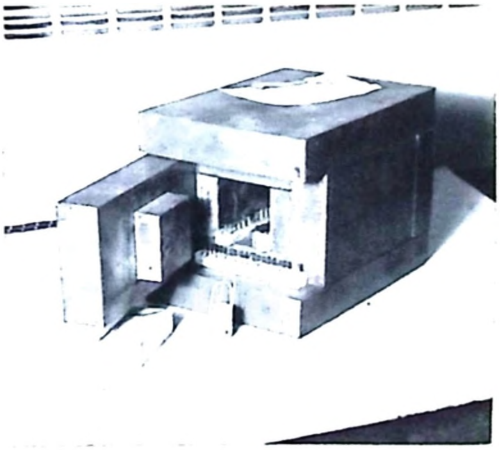

Figure 16 Storage Container

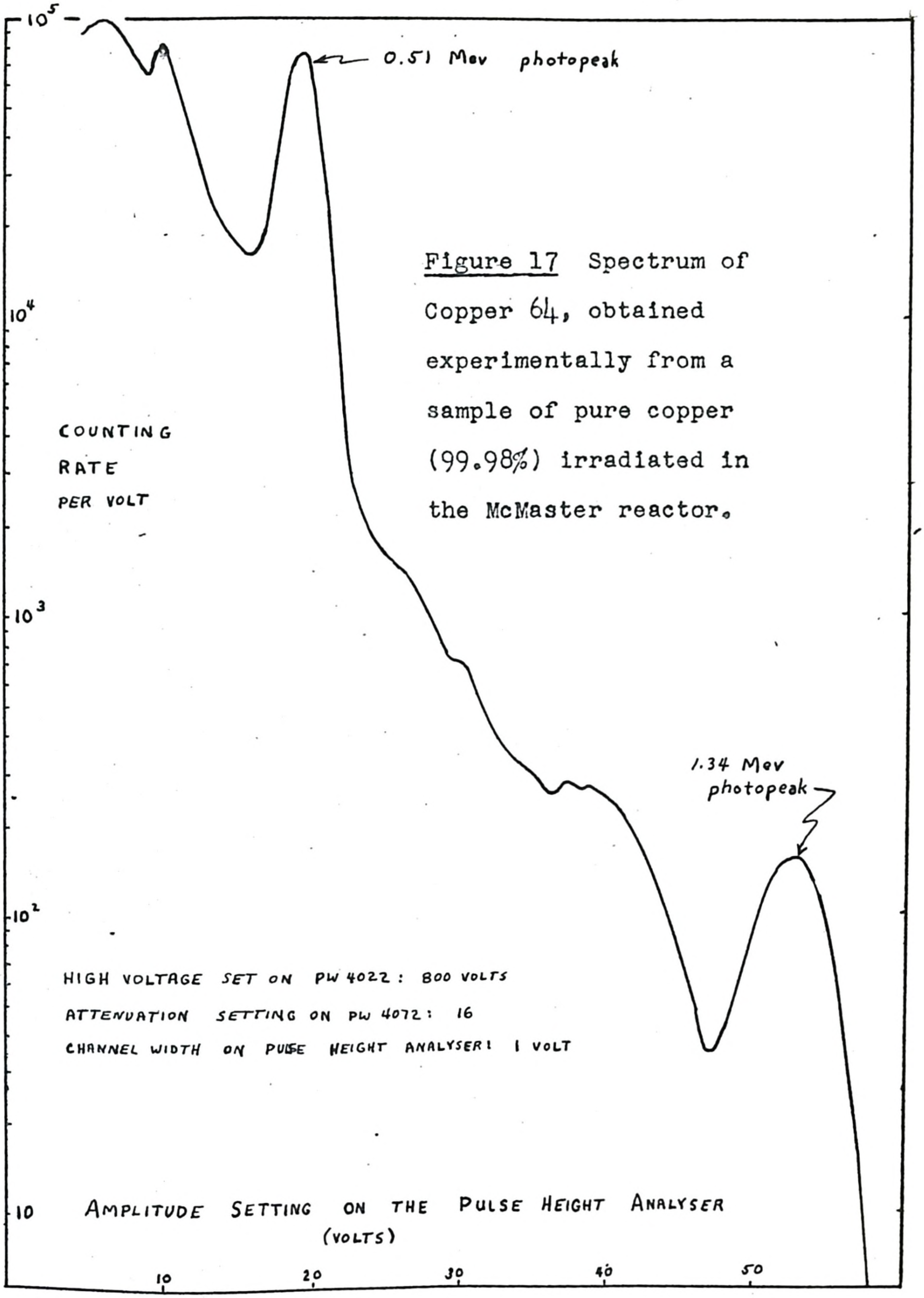

<u>Figure 17</u> Spectrum of Copper 64, obtained experimentally from a sample of pure copper (99.98%) irradiated in the McMaster reactor.

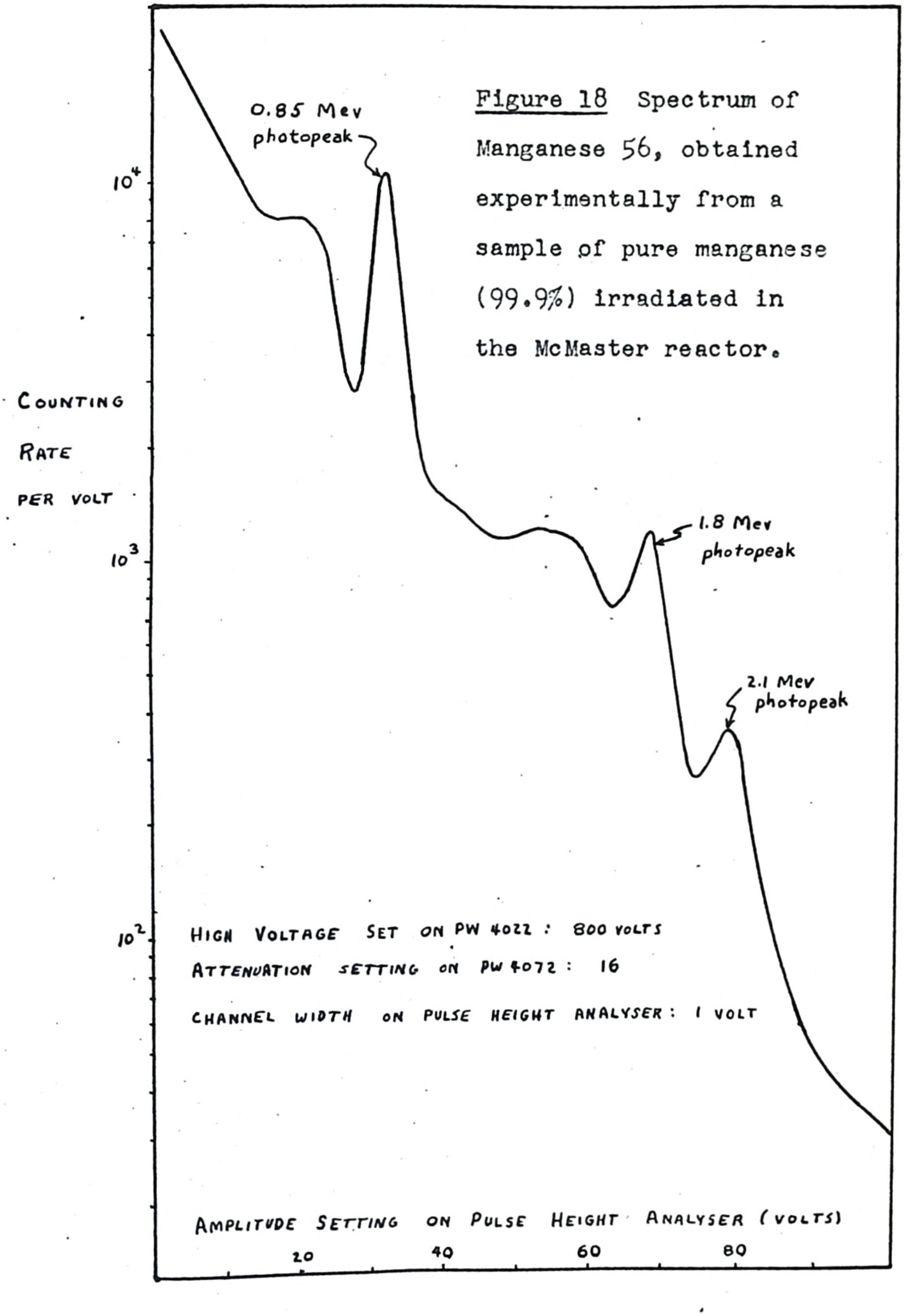

Figure 18 Spectrum of Manganese 56, obtained experimentally from a sample of pure manganese (99.9%) irradiated in the McMaster reactor.

HIGH VOLTAGE SET ON PW 4022 : 800 VOLTS

ATTENUATION SETTING ON PW 4072 : 16

CHANNEL WIDTH ON PULSE HEIGHT ANALYSER : 1 VOLT analysis. Since activated aluminum has a half-life of only 2.3 minutes and the other naturally-occurring copper isotope, Cu^{63}, has a half-life of 5.1 minutes when activated, these activities decay quickly and do not interfere with the measurements.

Some preliminary calculations were made to show the plausibility of the method of analysis. These calculations were based on a 24-hour irradiation in a flux of 1×10^{13} n/cm^2 - sec of 10 milligram samples of aluminum alloy containing four percent copper and one percent manganese. The count rates were calculated for samples in the base position of the lucite box within the counting castle. Equations (33) and (34) were used in these calculations; the calculated count rates and data used in these equations, other than those shown in Table 1, are shown in Table 2.

It is noted from Table 2 that the time required for a count of the manganese activity appears to be reasonable while that for the 0.51 Mev Cu peak is rather short and that for the 1.34 Mev Cu peak is somewhat long. Thus, by measuring the activities of the Cu 0.51 Mev gamma photopeak and of the Mn 1.80 Mev gamma photopeak, the counting rates appeared to be large enough to give accuracies of one percent within a reasonable time.

TABLE 1

Nuclear Data[17,18] for Cu, and Mn

Element	Cu	Mn
Isotope measured	63	55
Percent abundance	69.0	100
Atoms of isotope per gram of element, N_0	0.660×10^{22}	1.094×10^{22}
Thermal neutron cross section, σ barns	4.4	13.3
Half-life of activated isotope ($T_{1/2} = .693/\lambda$)	12.8 hr.	2.58 hr.
Saturation Activity in 1 gram of element in flux of 1×10^{13} n/cm^2-sec, dis/sec	2.90×10^{11}	1.468×10^{12}
Fraction of saturation activity attained in 24 hours of irradiation. ($1 - e^{-\lambda t_0}$)	.73	0.99
Decay factor for 10 hours	0.58	.068
Decay factor for 24 hours	0.274	0.00160
Energies of gamma rays emitted, in Mev, (percent of disintegrations)	1.35(0.5)	0.845(100); 1.81(30); 2.13(20)

TABLE 2

Expected counting rates from irradiated samples

Activities from 10 mg samples of 4% Cu, 1% Mn in Al, irradiated for 24 hours in a flux of 1×10^{13} n/cm^2-sec. Count rate observed with a 25 mm diameter NaI(Tl) crystal.

Isotope measured	Cu^{66}		Mn^{56}
Photopeak measured	0.51 Mev	1.34 Mev	1.80 Mev
Time of measurement after irradiation	24 hours		12 hours
Activity at time of measurement (disintegrations per second)	2.30×10^7		7.1×10^{-5}
g.p (see figure 7)	4×10^{-4}	1×10^{-4}	7.1×10^{-5}
Count rate (per second)	9.2×10^3	11	124
Time for 10^4 counts (one percent accuracy)	1 sec	910 secs	81 secs

EXPERIMENTAL PROCEDURE AND RESULTS

In order to provide some working data for the analysis of concentration-dependent ternary alloy diffusion and to test the suitability of activation analysis for diffusion measurements it was decided to examine the diffusion of manganese and copper in aluminum for the single-phase region in the aluminum-rich corner of the ternary diagram for this system, in addition to determining whether a manganese gradient has any effect upon the diffusion of copper in aluminum.

While the main experiments reported here were done at 556.5°C, the only ternary diagram available in the Al-rich corner is the 500°C isotherm[19]. The portion of this isotherm showing the extent of the Al α -phase at 500°C is reproduced as figure 19. From the binary phase diagrams[19] for Al-Cu and for Al-Mn, reproduced as figures 20 and 21 respectively, a rough extrapolation of the extent of the α -phase was made to the 556.5°C isotherm; the extrapolation is shown as figure 22. Rather than make up new alloys with compositions such that they lay entirely within the α -phase at the aluminum rich corner for this system, it was decided instead to use some available alloys even though the manganese content was higher than that for complete solubility. It is estimated that at least a full months delay would have been incurred had new alloys been made up and, because of the lack of experience in alloy making and of proper facilities at the university at the time, it was questionable whether the new alloys would have been as sound and as well homogenized as the ones available. The only disadvantage of the available alloys was that their manganese content was too high for complete solid solubility in the aluminum.

The compositions of alloys available for diffusion are shown in table 3.

TABLE 3

Composition of Alloys Available for Diffusion

(The concentrations in weight percent are shown for elements in the aluminum)

Alloy	Cu	Mn	Si	Mg	Fe
A	.003%	--	.001%	.001%	.003%
M	.004	1.18%	.01	.01	.01
C	4.00	--	.01	.01	.01
B	3.95	1.15	.01	.01	.01

Couples were made up of combinations of each one of these alloys with each of the others - to give a total of six different couples.

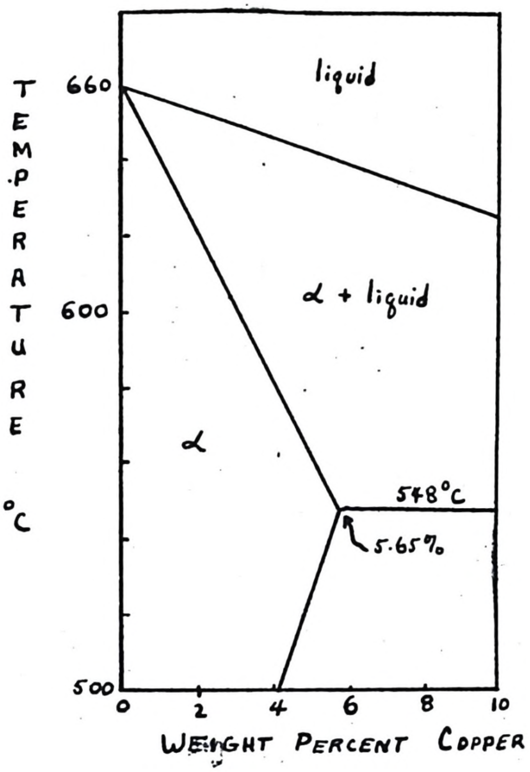

Figure 20 Binary Diagram for Aluminum-Copper

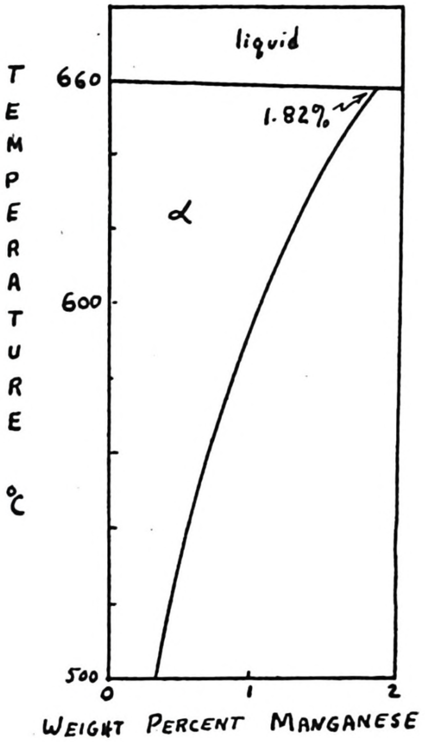

Figure 21 Binary Diagram for Aluminum-Manganese

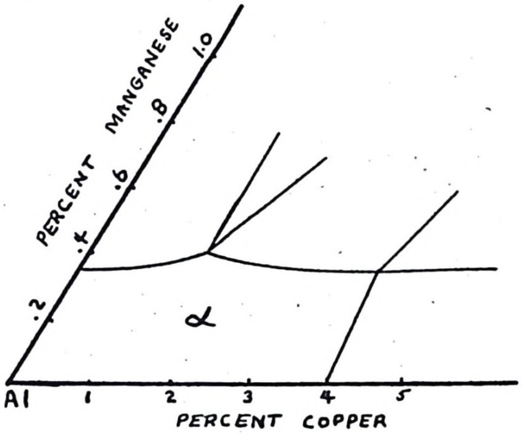

Figure 19 500°C Isotherm for the Al-rich corner of the Al-Cu-Mn system

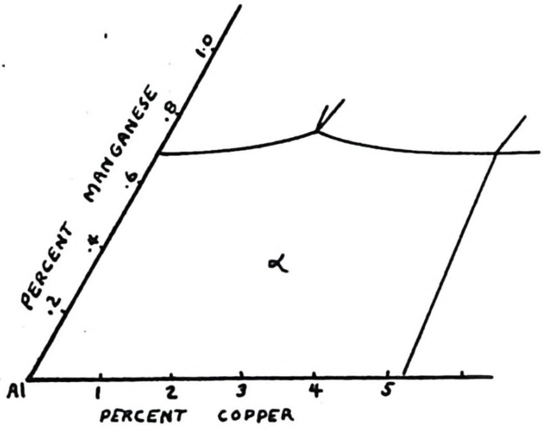

Figure 22 Extrapolated 556.5°C Isotherm for the Al-rich corner of the Al-Cu-Mn system

To make up the diffusion couples, cylinders of the alloys about one-half inch in diameter and about one-half inch long were machined in a 9 inch South-Bend Precision Lathe. In order to reduce the amount of oxide at the interface between the two halves of a couple, the surfaces of the halves to be placed together were given a final cut before being clamped tightly together in the 15-position clamp shown in figure 23. The time between the start of the final cut on the first half of a couple and the clamping of the two halves together was approximately 80 seconds in each case; this time was kept to a minimum to reduce the amount of oxide formed on the interface. The deformation produced at the interface because the halves of the couple were clamped tightly would tend to break up any oxide that did form, so that a sound weld between the two halves was made when the couple was heated to a high temperature. A platinum-platinum 10% rhodium thermocouple, certified by the U.S. National Bureau of Standards, was clamped between a dummy couple in one of the spare positions of the clamp and a metal sheet placed around the sides of the clamp to keep all the couples as close to the same temperature as possible. The clamped assembly was then placed in a forced-convection tempering oven, produced by the Blue M Electric Company, Model No. CW-1412, and pictured in figure 24.

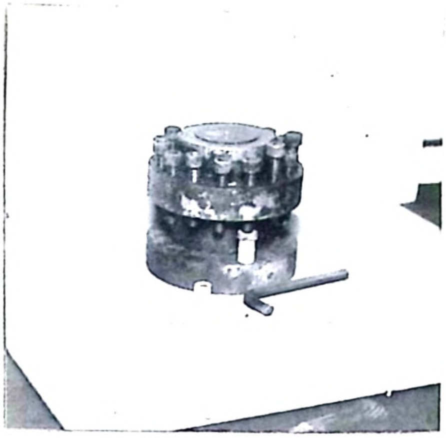

Figure 23 Clamp for Diffusion Couples

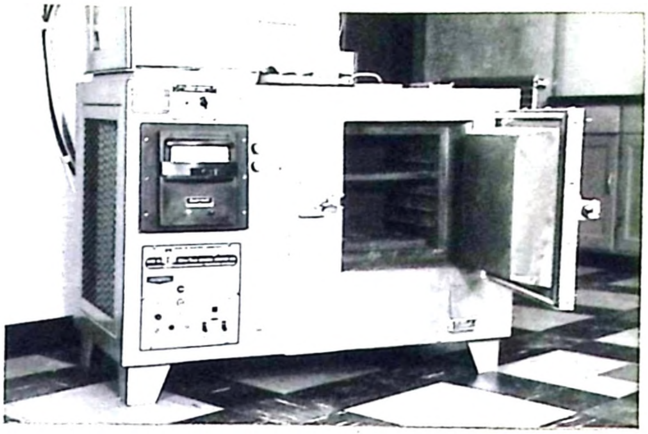

Figure 24 Forced-Convection Tempering Oven Used for Diffusion Anneals

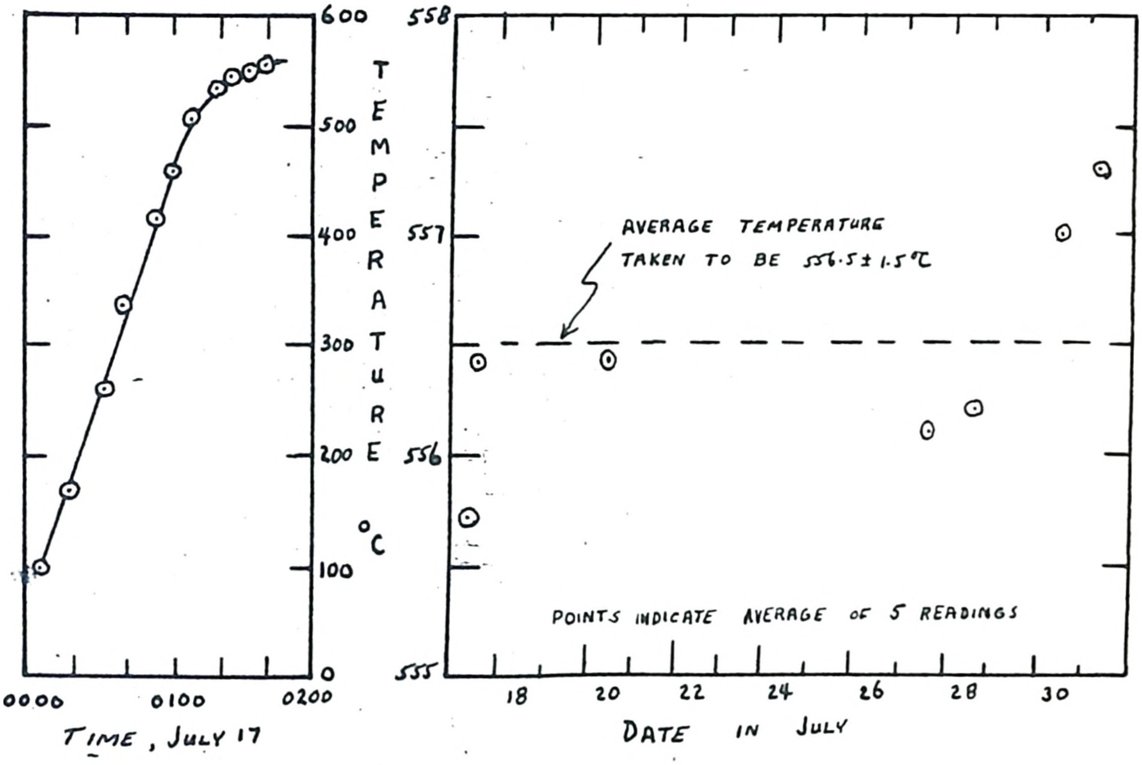

Figure 25 Diffusion Couple Temperature - measured with a platinum - platinum 10% rhodium thermocouple.

In order to get maximum diffusion penetration without liquid formation (see the Al-Cu phase diagram, figure 20) it was decided to anneal the samples at 560°C. Once the setting was made on the furnace, however, it was not altered, and the actual average temperature was 556.5°C ± 1.5% C. Readings of the temperature of the couples are plotted in figure 25. The time at temperature was 14 days and 8 hours ± 1 hour, or 1.238 ± .004 x 10^6 seconds.

Preparation of samples for irradiation

On removal from the Blue M oven, the clamp assembly with the couples in place was immediately water quenched so that it could be handled. The couples were then removed from the clamp; all seemed to be properly welded and this was verified by the fact that none of the couples broke apart when machined.

The couples were turned down to between 1.0 and 1.1 centimeter in diameter and lined up in a collet until it was thought that the interface was perpendicular to the center line of the lathe bed within about a thousandths of an inch. The lining-up was done by first etching the partially-turned couple for a few seconds in Tuckers etch (15 ml HF, 45 ml HCl, 15 ml HNO_3, and 25 ml H_2O) so that the interface could be seen. The couple was then placed in a lathe collet, checked for correct alignment with a fine pointer and a magnifying eye-piece, and, if necessary, adjusted. The lining-up procedure was rather tedious and took approximately two hours per couple.

Based on a microhardness scan on a couple diffused and examined earlier and on experimental data given by Smithells[20], it was decided to take samples out to a distance of 66 thousandths of an inch on either side of the interface. Cuts were made at intervals of 2 thousandths of an inch and those samples at mean distances of 1, 3, 5, 7, 9, 11, 15, 19, 25, 33, 43, and 55 thousandths of an inch on either side of the interface were set aside for activation analysis. The others were saved as a precaution against loss of the main samples.

Samples of from six to ten milligrams were weighed on a Mettler Type B6 Analytical Balance having an accuracy of ± .02 milligrams in the range used. The samples, originally in the form of machine turnings were then broken up and packed into individual silica capsules. Some of these capsules are shown in figure 26; each weighed about 100 milligrams, was about 18 millimeters long, had an inner diameter greater than one millimeter and an outer diameter between two and two and a half millimeters. The filled capsules were then sealed off with a gas torch, weighed for the purpose of identification in the case of any mix-up, and then placed in specific positions in a super-purity aluminum (99.99%) spacer machined for the purpose. Capsules containing standard

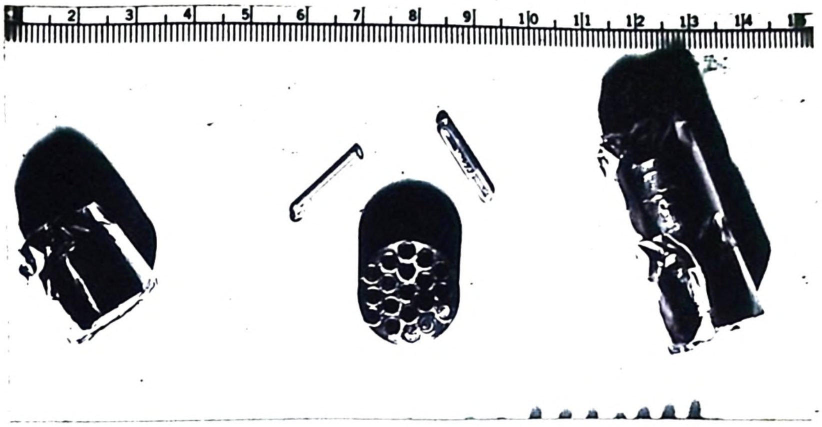

Figure 26 Silica capsules, filled and unfilled; irradiation spacer containing three capsules; and sample assemblies wrapped for irradiation.

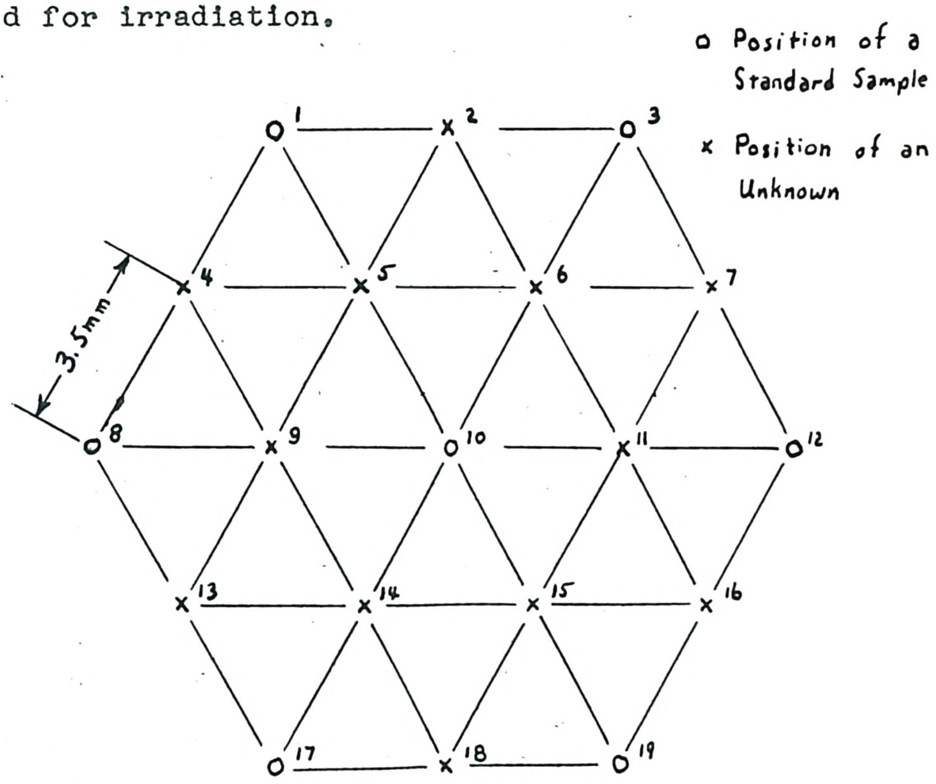

Figure 27 Spacing of capsules in irradiation container.

samples of the 3.95 percent Cu and 1.15 percent Mn were also made up in the same way. The relative positions of unknown samples and of standard samples are shown in figure 27. It is seen that twelve unknown samples and seven standard samples could be placed in each spacer. Thus, one spacer contained all the samples from one side of a diffusion couple. The two sides were packed separately in foil and then packed together end-on-end. The outer dimensions of the package for irradiation had to be less than 0.74 inches in diameter and 1.68 inches long since these were the inside dimensions of the irradiation can used for irradiations in the facility at Brookhaven National Laboratories.

Although the use of very pure aluminum capsules was considered, it was found that the silica glass capsules could be packed more easily, sealed better, cleaned more easily after an irradiation if contaminated on the outside, and had a lower background count. The silica glass was, of course, more susceptible to breakage; a few were broken during the packing procedure and three were found broken in the spacers on their return after the irradiation, but none broke as a result of an accidental fall to the floor.

Measurement of activity of the samples

The 24-hour irradiation of a package of samples at the Brookhaven reactor in New York was completed in the morning and shipped by air express to Malton airport. The isotopes were shipped inside a two-inch-wall lead container, which in turn was contained in a wooden box about two-feet on the side. The isotopes were picked up by car at the airport and brought back to the university.

When the isotopes reached the university, they were taken to the Radio-Isotopes Laboratory in the Nuclear Research Building and unpacked behind a temporary two-inch brick wall, under a fume hood. By this time it was usually about twelve hours after the package had been removed from the reactor but there was still between 100 and 200 millicuries of activity present and the dose-rate from the package was about 400 milliroentgens at an unshielded distance of one foot. In order to remove any loose contamination from the outside of the capsules they were washed individually under a stream of tap water and wiped with two separate pieces of Kleenex. The second piece of Kleenex was checked for activity by placing it next to a sensitive counter. If the Kleenex had picked up any activity, the capsule was re-wiped; otherwise it was put into its correct position in an aluminum cylinder with holes drilled in it to accomodate the capsules. This cylinder was similar to the one used to space the capsules during an irradiation. When the aluminum cylinder was filled, it was taken to the counting room inside a lead carrying container. The samples were transferred to a tray for ease of handling and placed inside the lead storage container shown in figure 16 until they were to be counted.

All of the counting was done using a photomultiplier voltage of 800 volts (set on the high voltage unit PW 4022) and an attenuation setting of 16 on the linear amplifier PW 4072.

The manganese activity of each sample was determined first by counting the 1.80 Mev photopeak, which was usually centered around 70 volts on the pulse height analyser with the above settings on PW 4022 and PW 4072. Once the position of this photopeak had been determined more precisely, the amplitude setting on the pulse height analyser was fixed and a first run made of the manganese activity using a channel width of 4 volts and with the samples on shelf number 10 of the lucite box inside the counting castle. For a count of 1 x 10^4 the counting time per capsule was usually from two to six minutes and the total time required to count the activity in 38 capsules was from two to four hours. Whenever there was an appreciably smaller count rate for a given capsule, the number of counts taken was reduced so that the total counting time was approximately the same for all capsules.

In order to count the manganese activity of each capsule a second time the capsules were moved closer to the detecting crystal by placing them in shelf position seven; also the channel width was increased to eight volts. With the samples on shelf seven and a channel width of eight volts, the observed counting rate was roughly the same as it was three hours earlier using a channel width of only four volts and with the samples on shelf ten. The position of maximum count (photopeak position) was then checked and a run made similar to the first.

Although the voltage setting for the photomultiplier tube was unchanged throughout the final experiments the very small fluctuations in the voltage supply resulted in noticeable changes in amplification by the photomultiplier tube; consequently, the position of the photopeak on the pulse height analyser was found to drift appreciably even in an hour. For this reason it was found best to take several readings of counting rate for each sample at slightly different amplitude settings as close as possible to the photopeak position. Provided that a maximum was observed in the counting rate at some amplitude setting within the range scanned then one could be certain that the center of the photopeak was at the amplitude for which the highest rate was observed. Unless the photopeak rate was observed, then the counting rate would be appreciably less; the error would be greater the further an amplitude setting was from the actual photopeak position. With the manganese samples on shelf number ten and a channel width of four volts the count rate was usually not fast enough to permit this short scan on each sample before the activity died away. However, with the settings for the second manganese run it was sometimes possible.

The copper activity of the samples was measured by counting the 0.51 Mev annihilation gamma ray (see figure 17). With the sample on shelf number thirteen and a channel width of four volts the counting was still very high a day after the irradiation. It was therefore fairly easy to make individual scans (usually counts were taken at 0.2 volt intervals of the amplitude setting) to check the photopeak position with each sample, and to make two complete runs in this way.

Results of the activity measurements

The steps followed when calculating the weight percentage of an isotope in a sample from the measured activity are listed below:

(a) The uncorrected counting rate, Au, for each sample was calculated using the relation

$$A_u = \frac{C}{\omega \Delta T} \tag{35}$$

where C = the number of counts taken at the photopeak position

ΔT = the time interval required for C counts to be taken

and ω = the weight of the sample

(b) A background correction, B, was made for impurity activity in the samples and, in the case of the copper, for any appreciable manganese activity that still existed. The background corrections were determined from couples A - M and A - C (see table 3) for the copper and manganese respectively; and the results are shown in figures 28 and 29. It was felt permissible to apply the background activities obtained from these couples to other couples since all samples were irradiated in the same facility of the Brookhaven reactor and at the same reported flux. An activity, corrected for background, was thus obtained for each sample from the relation

$$A_c = A_u - B \tag{36}$$

(c) Having determined the corrected activity at the time of a measurement, then the activity was calculated at some arbitrary mean time for the measurements on a set of samples using the known decay constant for the copper or manganese isotope tabulated in Table 1. Thus, the activity per milligram for each sample of a nineteen-sample assembly was determined for a particular time from the equation

$$A = A_c e^{\lambda \tau} \tag{37}$$

where λ = the decay constant tabulated in Table 1

τ = time as measured from the arbitrary mean time

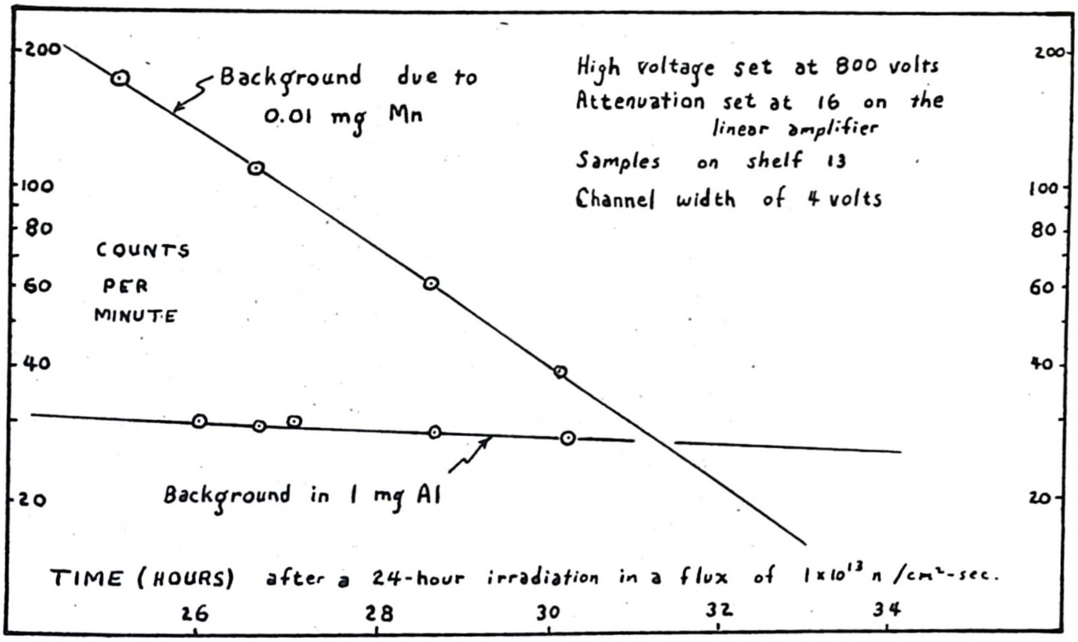

Figure 28 Background in samples at the 0.51 Mev Copper Photopeak.

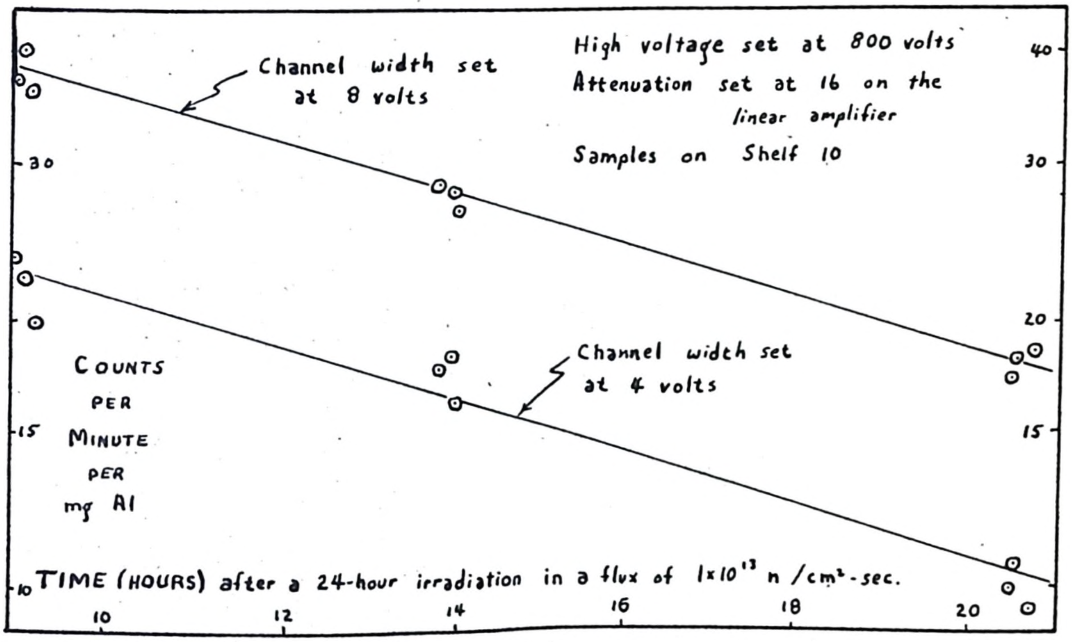

Figure 29 Background in samples at the 1.8 Mev Manganese Photopeak.

for a given set of measurements

A_c = the corrected activity per milligram of sample at the time τ

(d) From the activities of the standard samples in adjacent positions, the standard activity for a position containing a sample of unknown composition was determined by linear interpolation.

(e) From the standard activity interpolated for a position containing a sample of unknown composition, and the weight percent of the measured isotope known to exist in the standard samples the weight percent of isotope in the unknown sample was calculated from the equation

$$W = \frac{A}{A'} W' \qquad (38)$$

where A = the corrected activity per milligram of unknown sample, for a particular time

A' = the corrected standard activity per milligram , at the particular time, interpolated for the position of the unknown

W' = the weight percent of isotope known to exist in the standard sample

W = the calculated weight percent of isotope in the unknown sample

A typical result is shown in Table 4 for the weight percent of copper determined in an unknown sample.

TABLE 4

Typical Results for the Calculation of the Weight Percent of an Isotope in a Sample

Sample	Weight w mg	Counts C	Time Interval ΔT	Uncorrected Rate A_u	Background B
A 10	7.09	4×10^4	.370	1.528×10^4	.032
A 11	8.51	4×10^4	.439	1.071×10^4	.004
A 12	8.06	4×10^4	.330	1.502×10^4	.032

Sample	Corrected Rate A_c	τ minutes	Activity A	Standard Activity A^1	Weight Percent W
A 10	1.496×10^4	-1	1.495×10^4	--	--
A 11	1.067×10^4	2	1.069×10^4	1.487×10^4	2.84
A 12	1.470×10^4	5	1.478×10^4	--	--

Note: The weight percent of isotope in the standard samples, W^1, was 3.95. The standards contained manganese which still had appreciable activity whereas the unknown sample did not; hence, the larger background correction, B, for the standards.

The results of the copper concentration determinations for each couple are plotted in figures 30 and 31, while those for the manganese are shown in figure 32. It is to be noted that the curves all appear to be symmetric, indicating no dependence of the diffusion coefficients upon concentration and, also, that no cross-effect is obvious from figures 30 or 32. Consequently, curves for a constant diffusion coefficient were fitted to the results shown in each of these figures and no attempt was made to determine a different coefficient for different couples. The solid curve drawn in for the copper penetration was fitted to the results obtained from the C-A couple (4 percent copper in aluminum versus pure aluminum) using equation 5; the diffusion coefficient found to give the best fit was 1.78×10^{-9} cm^2/sec. The curve for the manganese penetration was fitted to the B-C couple (3.95 percent copper plus 1.15 percent manganese in aluminum versus 4.00 percent copper in aluminum); the diffusion coefficient obtained was 9.0×10^{-12} cm^2/ sec. Discrepancies between the drawn curve and points from couples other than that for which the curve was fitted would be due, in part, to differences in the end concentrations. Except for the absence of a concentration dependence in the diffusion coefficient obtained for copper, these results are in good agreement with those given by Smithells[20]. The result obtained for the manganese coefficient is probably for the lowest temperature

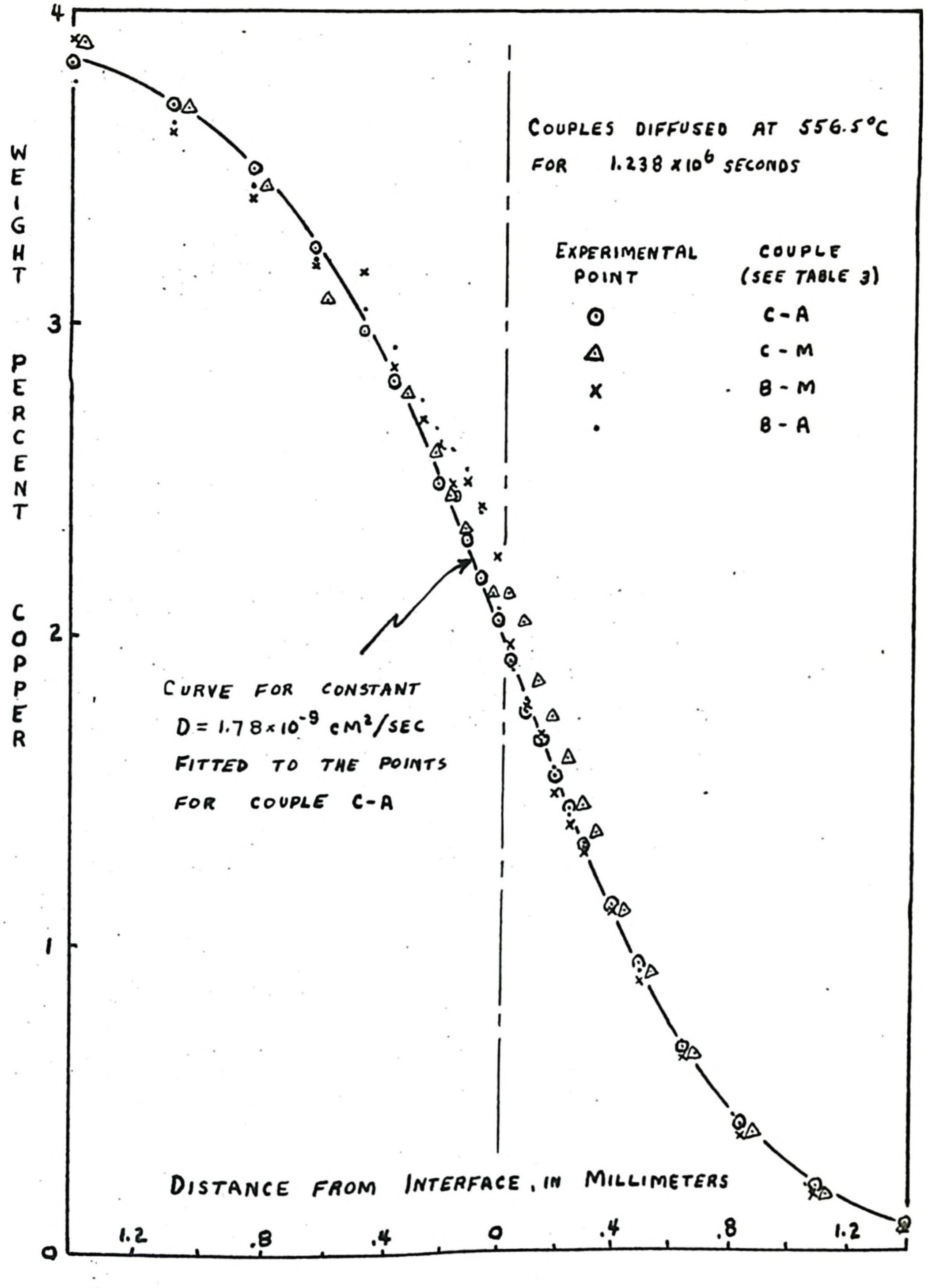

Figure 30 Copper Penetration in the Couples

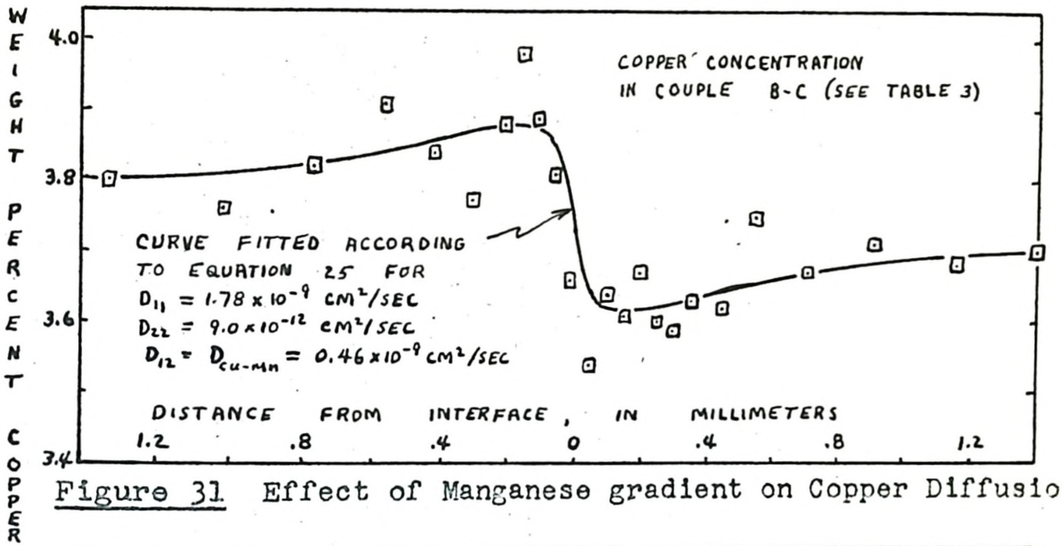

Figure 31 Effect of Manganese gradient on Copper Diffusion

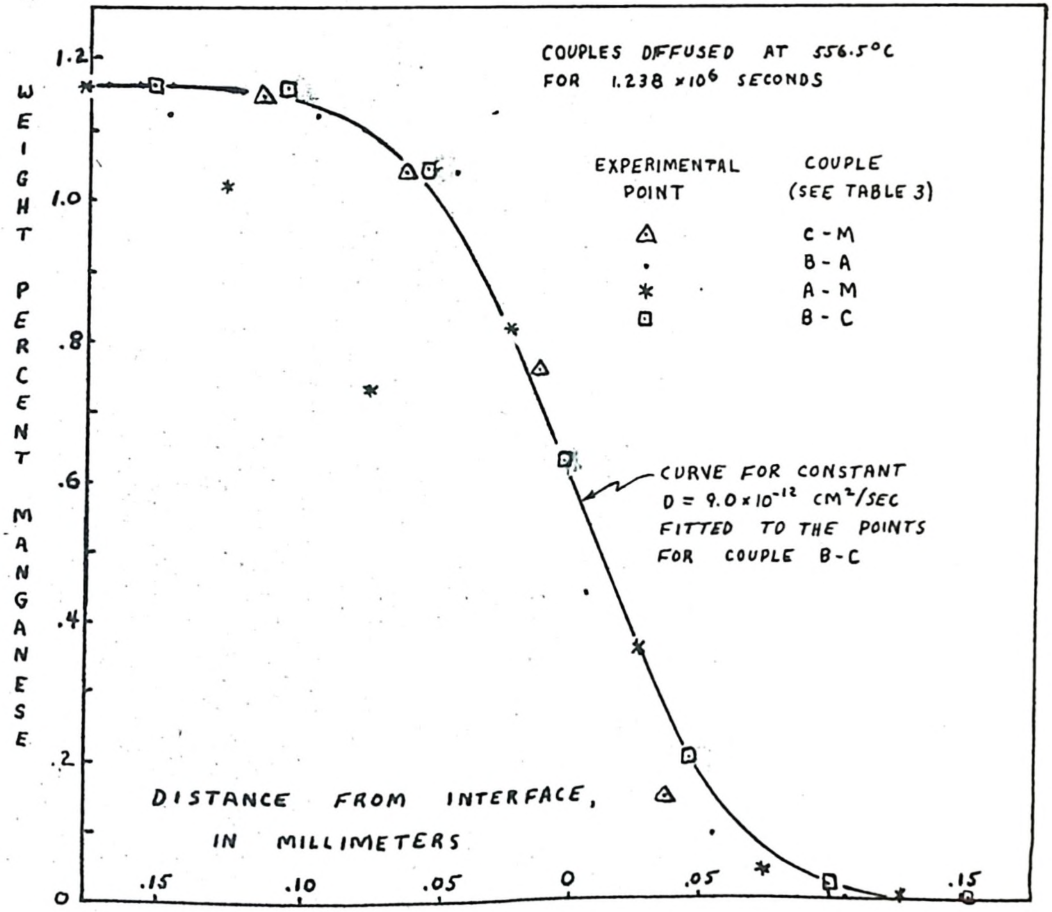

Figure 32 Manganese Penetration in the Couples

at which manganese diffusion has been measured.

The results shown in figure 31 indicate the strong effect a manganese concentration gradient has upon the diffusion of copper in aluminum. Again, no concentration dependence was discernable so that equation 25, for constant coefficients, was used to fit a curve to the experimental results. Using the values of $D_{11} = 1.78 \times 10^{-9}$ cm^2/sec obtained for the copper diffusion coefficient and $D_{22} = 9.0 \times 10^{-12}$ cm^2/sec obtained for the manganese diffusion coeficient, an off-diagonal coefficient, $D_{12} = 0.46 \times 10^{-9}$ cm^2/sec was found to give a good fit. It is noted that this is more than one-quarter of the on-diagonal coefficient, D_{11}, and hence that the cross-effect is large.

Discussion

In general, the manganese determinations were not as precise as those for the copper. This was mainly because the manganese activity in the samples, when received about ten hours after an irradiation at the Brookhaven National Laboratories, was not as high as the copper activity. This situation will improve at this university when the McMaster reactor becomes fully operational, and activities can be measured shortly after an irradiation. In addition, however, because manganese activity decays more rapidly than the copper activity measured, there is not as much time to make the activity measurements.

For the 0.51 Mev photopeak of copper, it was found that when the amplitude setting on the pulse height analyser was different from the actual photopeak position by 0.2 volts, the counting rate was reduced by 0.5 percent; this reduction in counting rate becomes greater as the discrepancy between photopeak position and amplitude setting increases. Consequently, it was essential that the actual photopeak position be known at all times. With the high copper activity, it was easy to check the 0.51 Mev photopeak by taking readings at 0.2 volt intervals about the photopeak position. For the manganese 1.8 Mev peak the same type of error occurs, and it was found best to move the samples closer to the crystal to obtain counting rates high enough for the photopeak position to be checked. Errors due to slight differences in geometry for different samples would increase; but this error was only of the order of one percent for samples in shelf position eight, whereas errors due to an undetected shift in photopeak position could amount to about ten percent.

The stock metals from which the couples were machined were homogeneous microscopically. However, the differences in end concentrations observed for couple sides that came from the same stock metal indicate at least a slow variation in concentration of solute throughout the stock metal. For this reason it is advisable to use as standards, samples machined from the ends of the pieces used in a couple, and to have a wet chemical analysis done on a large sample as a check on the composition of the standard samples.

In order to do a neutron activation analysis for an element it is desirable that the element have an appreciable cross-section for thermal neutrons ($>$ 0.1 barns), that it emit high energy gamma radiation in most of its disintegrations, and that it have a half-life of at least a few hours. When the concentrations of two elements are to be determined for the same sample then there must be some way of measuring the activities independently. One such method is that found for the copper-manganese-aluminum system. The important features of this system are:

(i) The aluminum activity decays relatively quickly and so does not, in itself, interfere with the activity measurements on manganese and copper.

(ii) The copper gamma-ray spectrum drops off sharply at an energy below that of a measureable manganese gamma-ray photopeak. This feature permits the manganese activity to be determined free from interference from the copper activity.

(iii) The manganese half-life is only 2.58 hours compared with 12.8 hours for the copper. Thus, the copper determinations can be made without interference from the manganese by waiting about 24 hours after an irradiation to allow the manganese activity to decay.

Thus, provided there is sufficient activity, the concentrations of two or more elements in the same sample can be determined whenever the element with a shorter half-life emits gamma radiation of energy higher than any of those for the longer-lived element or elements.

Because of the effect a manganese concentration gradient has upon the diffusion of copper in aluminum, the presence of manganese in a solution of copper in aluminum will affect the precipitation rate of $CuAl_2$. When a precipitate of $CuAl_2$ forms, it grows with a depletion of copper from the surrounding metal. Manganese will be pushed outwards from the precipitate as it grows so that the copper will have to diffuse against a manganese concentration gradient. However, according to the results obtained, the opposing manganese gradient will actually increase the rate of copper diffusion to the precipitate. Thus the presence of manganese in a solution of copper in aluminum will increase the rate of precipitation of $CuAl_2$.

Although the sides of the couple originally containing manganese contained over one percent manganese, the amount of manganese in actual solution in the α-phase of the aluminum would only be about 0.7 percent (see figure 21). The remainder would exist as a precipitate, which would not interfere with the diffusion of either copper or manganese but would maintain the amount of manganese in solution at 0.7 percent until the precipitate was depleted.

CONCLUSIONS

1. An accuracy of one percent with samples of the order of ten milligrams is feasible for the determination of copper concentration in aluminum. The same precision can be obtained with manganese provided the activity is measured within a few hours of an irradiation.

2. There is no concentration dependence of diffusion in the aluminum-rich α-phase of the aluminum-copper-manganese system, within five percent.

3. The diffusion coefficients of copper and manganese in aluminum at 556.5°C are 1.78×10^{-9} cm^2/sec and 9.0×10^{-12} cm^2/sec respectively. The off-diagonal coefficient for the effect a manganese gradient has upon the rate of diffusion of copper in aluminum is 0.46×10^{-9} cm^2/sec.

4. The presence of manganese in a solution of copper in aluminum will increase the rate of precipitation of $CuAl_2$.

APPENDIX A

Relationships between ternary diffusion coefficients for different reference frames, for $\Sigma C=$ constant and $\Sigma J=0$

The three diffusion currents in a ternary system, written out with full consideration given to all gradients, are

$$(A\text{-}1)\quad \left\{\begin{aligned} J_1 &= -D'_{11}\frac{\partial c_1}{\partial x} - D'_{12}\frac{\partial c_2}{\partial x} - D'_{13}\frac{\partial c_3}{\partial x} \\ J_2 &= -D'_{21}\frac{\partial c_1}{\partial x} - D'_{22}\frac{\partial c_2}{\partial x} - D'_{23}\frac{\partial c_3}{\partial x} \\ J_3 &= -D'_{31}\frac{\partial c_1}{\partial x} - D'_{32}\frac{\partial c_2}{\partial x} - D'_{33}\frac{\partial c_3}{\partial x} \end{aligned}\right.$$

Using the relations $\Sigma C=$ constant and $\Sigma J=0$ these three equations involving nine coefficients may be reduced to two equations with only four coefficients. However, there are three possible reference frames, each corresponding to the consideration of one of the three components in turn as the solvent component and each resulting in two equations with four diffusion coefficients. Since any one of these three groups of four coefficients can be used to describe diffusion phenomena in the same ternary system it must be possible to relate the four coefficients from one reference frame to the four from either one of the other two. The necessary relationships are derived below.

By applying the relation $\sum C = \text{constant}$ to equations (A-1) one can obtain

(a) from $C_3 = \text{constant} - C_1 - C_2$; $\frac{\partial C_3}{\partial x} = -\frac{\partial C_1}{\partial x} - \frac{\partial C_2}{\partial x}$:

$$\text{(A-2)} \quad \left\{ \begin{array}{lll} J_1 = -D_{11}^{3}\frac{\partial C_1}{\partial x} - D_{12}^{3}\frac{\partial C_2}{\partial x} & \text{where} & D_{11}^{3} = D_{11}' - D_{13}' \\ & & D_{12}^{3} = D_{12}' - D_{13}' \\ J_2 = -D_{21}^{3}\frac{\partial C_1}{\partial x} - D_{22}^{3}\frac{\partial C_2}{\partial x} & \text{where} & D_{21}^{3} = D_{21}' - D_{23}' \\ & & D_{22}^{3} = D_{22}' - D_{23}' \end{array} \right.$$

(The ternary diffusion coefficient D_{ik}^{m} refers to the diffusion of component i down the gradient of component k when the gradient of component m has been removed from consideration in the system; component m is considered as the solvent component).

(b) from $\frac{\partial C_2}{\partial x} = -\frac{\partial C_1}{\partial x} - \frac{\partial C_3}{\partial x}$

$$\text{(A-3)} \quad \left\{ \begin{array}{lll} J_1 = -D_{11}^{2}\frac{\partial C_1}{\partial x} - D_{13}^{2}\frac{\partial C_3}{\partial x} & \text{where} & D_{11}^{2} = D_{11}' - D_{12}' \\ & & D_{13}^{2} = D_{13}' - D_{12}' \\ J_3 = -D_{31}^{2}\frac{\partial C_1}{\partial x} - D_{33}^{2}\frac{\partial C_3}{\partial x} & \text{where} & D_{31}^{2} = D_{31}' - D_{32}' \\ & & D_{33}^{2} = D_{33}' - D_{32}' \end{array} \right.$$

and, (c) from $\frac{\partial C_1}{\partial x} = -\frac{\partial C_2}{\partial x} - \frac{\partial C_3}{\partial x}$

$$\text{(A-4)} \quad \left\{ \begin{array}{lll} J_2 = -D_{22}^{1}\frac{\partial C_2}{\partial x} - D_{23}^{1}\frac{\partial C_3}{\partial x} & \text{where} & D_{22}^{1} = D_{22}' - D_{21}' \\ & & D_{23}^{1} = D_{23}' - D_{21}' \\ J_3 = -D_{32}^{1}\frac{\partial C_2}{\partial x} - D_{33}^{1}\frac{\partial C_3}{\partial x} & \text{where} & D_{32}^{1} = D_{32}' - D_{31}' \\ & & D_{33}^{1} = D_{33}' - D_{31}' \end{array} \right.$$

It is seen from the auxiliary relations between the D_{ik}^{m} and the D_{ik}' that

$$\text{(A-5)} \quad \begin{cases} D_{12}^{3} = D_{12}' - D_{13}' = -D_{13}^{2} \\ D_{23}^{1} = D_{23}' - D_{21}' = -D_{21}^{3} \\ D_{31}^{2} = D_{31}' - D_{32}' = -D_{32}^{1} \end{cases}$$

and

$$\text{(A-6)} \quad \begin{cases} D_{11}^{3} - D_{11}^{2} = D_{12}' - D_{13}' = D_{12}^{3} \\ D_{22}^{1} - D_{22}^{3} = D_{23}' - D_{21}' = D_{23}^{1} \\ D_{33}^{2} - D_{33}^{1} = D_{31}' - D_{32}' = D_{31}^{2} \end{cases}$$

However, equations (A-5) and (A-6) are not sufficient to relate all the diffusion coefficients for one reference frame to those for another. To do this, some relation between the diffusion currents must be used. By taking $\Sigma J = 0$ the necessary set of equations can be obtained as follows.

Since $J_3 = -J_1 - J_2$, then from (A-2):

$$J_3 = (D_{11}^{3} + D_{21}^{3})\frac{\partial c_1}{\partial x} + (D_{12}^{3} + D_{22}^{3})\frac{\partial c_2}{\partial x}$$

Using $\frac{\partial c_1}{\partial x} = -\frac{\partial c_2}{\partial x} - \frac{\partial c_3}{\partial x}$ then

$$J_3 = -(D_{11}^{3} + D_{21}^{3} - D_{12}^{3} - D_{22}^{3})\frac{\partial c_2}{\partial x} - (D_{11}^{3} + D_{21}^{3})\frac{\partial c_3}{\partial x}$$

But from (A-4)

$$J_3 = -D_{32}^{1}\frac{\partial c_2}{\partial x} - D_{33}^{1}\frac{\partial c_3}{\partial x}$$

Therefore:

(A-7) $D_{33}^{1} = D_{11}^{3} + D_{21}^{3}$ and $D_{32}^{1} = D_{33}^{1} - D_{12}^{3} - D_{22}^{3}$

Also, using $\frac{\partial c_2}{\partial x} = -\frac{\partial c_1}{\partial x} - \frac{\partial c_3}{\partial x}$ then, again from (A-2):

$$J_3 = -\left(D_{12}^{3} + D_{22}^{3} - D_{21}^{3} - D_{11}^{3}\right)\frac{\partial c_1}{\partial x} - \left(D_{12}^{3} + D_{22}^{3}\right)\frac{\partial c_3}{\partial x}$$

$$\equiv D_{31}^{2}\frac{\partial c_1}{\partial x} - D_{33}^{2}\frac{\partial c_3}{\partial x} \qquad \text{from equation (A-3)}$$

Thus

(A-8) $D_{33}^{2} = D_{12}^{3} + D_{22}^{3}$ and $D_{31}^{2} = D_{33}^{2} - D_{21}^{3} - D_{11}^{3}$

Eight more equations, not all independent, can be obtained in a similar manner by starting with $J_1 = -J_2 - J_3$ in equation (A-4) and with $J_2 = -J_2 - J_3$ in equation (A-3).

The twelve equations can finally be grouped conveniently as follows:

$$\text{(A-9)}\quad \left\{\begin{array}{lllll} D_{12}^{3} & = D_{33}^{2} - D_{22}^{3} & = D_{11}^{3} - D_{11}^{2} & = -D_{13}^{2} \\ D_{23}^{1} & = D_{11}^{3} - D_{33}^{1} & = D_{22}^{1} - D_{22}^{3} & = -D_{21}^{3} \\ D_{31}^{2} & = D_{22}^{1} - D_{11}^{2} & = D_{33}^{2} - D_{33}^{1} & = -D_{32}^{1} \end{array}\right.$$

or, in general notation:

(A-10) $D_{ik}^{m} = D_{mm}^{k} - D_{kk}^{m} = D_{ii}^{m} - D_{ii}^{k} = -D_{im}^{k}$

Equations (A-9) would be useful when plotting the surface for a ternary diffusion coefficient. Since the component which is considered as the solvent is usually that which is present in the greatest amount it may be necessary to transfer data from experiments in which one component was considered as the solvent to a diagram which was begun for a diffusion coefficient for which a different component was considered as the solvent. Equations (A-9) provide the formulae for making such a transfer.

For example, to transfer data from the system in which component 3 is the solvent to the system in which component 2 is the solvent, one would use the formulae:

$$
\text{(A-11)} \quad \begin{cases}
D^{2}_{13} = -D^{3}_{12} \\
D^{2}_{11} = D^{2}_{13} + D^{3}_{11} \\
D^{2}_{33} = -D^{2}_{13} + D^{3}_{22} \\
D^{2}_{31} = D^{1}_{22} - D^{2}_{11} = D^{3}_{22} - D^{3}_{21} - D^{2}_{11} \\
(\text{or } D^{2}_{31} = D^{2}_{33} - D^{1}_{33} = D^{2}_{33} - D^{3}_{21} - D^{3}_{11})
\end{cases}
$$

The above considerations apply whether the Ds are functions of concentration or constant. The equations could thus be used to test the validity of an assumption of constant Ds for a particular ternary system (provided, of course, that the assumptions $\Sigma J = 0$ and $\Sigma C =$ constant are valid).

It is noted that off-diagonal coefficients should not be expected to have any particular sign since they are actually differences between two more fundamental diffusion coefficients, D'_{ik} and D'_{in} - the sizes of which should be comparable.

REFERENCES

1. Onsager, L., Ann. N. Y. Acad. Sci. 46, 241, (1945-46)
2. Darken, L. S., Atom Movements, A. S. M., Cleveland, (1951)
3. Kirkaldy, J. S., Can. J. Phys. 35, 435, (1957)
4. Kirkaldy, J. S., Can. J. Phys. 36, 899, (1958)
5. Kirkaldy, J. S., Can. J. Phys. 36, 907, (1958)
6. Kirkaldy, J. S., Can. J. Phys. 36, 917, (1958)
7. Kirkaldy, J. S., Can. J. Phys. 37, 30, (1959)
8. Boltzmann, L., Ann. Physik, Leipzig 53, 959, (1894)
9. Matano, C., Japan J. Phys. 8, 109, (1933)
10. Castaing, R. and Guinier, A., Anal. Chem. 25, 724 (1953)
11. Fick, A., Pogg. Ann. 94, 59, (1855)
12. Barrer, R. M., Diffusion in and Through Solids, Cambridge University Press, (1951), p. 9
13. Handbook of Chemistry and Physics, Chemical Rubber Publishing Co., Cleveland, (1948), p. 204
14. Smigelskas, A. D. and Kirkendall, E. O., Trans. A. I. M. E. 171, 130, (1947)
15. Fujita, H. and Gosting, L. J., J. Am. Chem. Soc. 78, 1099, (1956)
16. Miller, W. F., Reynolds, J. and Snow, W. J., Rev. Sci. Instr. 30, 141, (1959)
17. General Electric Company, Chart of the Nuclides, Knolls Atomic Laboratory, U. S. A. E. C., (1956)

18. Sullivan, W. H., Trilinear Chart of Nuclides, Oak Ridge National Laboratories, U. S. A. E. C. (1957)

19. Smithells, C. J., Metals Reference Book, vol. I, Butterworths (1955)

20. Smithells, C. J., Metals Reference Book, vol. II, Butterworths (1955)